INSTANTANEOUS OPTIMAL CONTROL LAWS FOR TALL BUILDINGS

UNDER SEISMIC EXCITATIONS

by

J. N. Yang,[1] A. Akbarpour[2] and P. Ghaemmaghami[3]

June 10, 1987

Technical Report NCEER-87-0007

NCEER Contract Number 86-3021

NSF Master Contract Number ECE 86-07591

and

NSF Grant No. ECE-85-21496

1 Professor, Dept. of Civil, Mechanical and Environmental Engineering, George Washington University
2 Graduate Research Assistant, Dept. of Civil, Mechanical and Environmental Engineering, George Washington University
3 NRC-NASA Residence Research Associate, Langley Research Center

NATIONAL CENTER FOR EARTHQUAKE ENGINEERING RESEARCH
State University of New York at Buffalo
Red Jacket Quadrangle, Buffalo, NY 14261

ABSTRACT

A critical review of classical optimal control algorithms is made with respect to the specific application of structural control under seismic loads. With the earthquake ground acceleration being the major source of continuous external disturbances, the Riccati closed-loop control does not satisfy the optimal condition. New optimal control algorithms are proposed herein, including the instantaneous optimal open-loop control, instantaneous optimal closed-loop control and instantaneous optimal closed-open-loop control. These new control algorithms are aimed at developing feasible control algorithms that can easily be implemented, for applications to seismic-excited structures. Numerical examples are worked out to demonstrate the control efficiency of the proposed control algorithms.

TABLE OF CONTENTS

TABLE OF CONTENTS (Continued)

iii

LIST OF ILLUSTRATIONS

LIST OF TABLES

SECTION 1

INTRODUCTION

Because of the potential pay-offs either in minimizing the catastrophic failure or in increasing the structural safety, intensive research efforts have been made for the possible application of active control systems to available civil engineering structures. In this regard, a large body of literature has been available [ref. 1-69]. It has been predicted that the next generation of buildings will be much taller and flexible. For these super-tall buildings to function safely under hostile environments, such as strong earthquakes or wind gusts, control systems, either passive or active, may conceivably become an integral part of the building.

It is remarkable to notice that there is a lack of experimental work or laboratory verifications of the analytical results for the active control of seismic-excited structures. Clearly, realistic experiments are needed to evaluate the feasibility and implementability of active control devices in practice. The critical importance of experimental studies in structural control has been emphasized by Yao and Soong [61]. Likewise, the experimental research efforts will reveal various aspects in which further analytical/numerical studies are needed.

An experimental program for the active control of model buildings subjected to earthquake excitations has been conducted at the State University of New York (SUNY) at Buffalo since 1984 with the participation of the George Washington University. During the course of such a collaborative experimental research, it was found that the active control laws available in the literature are quite limited for practical implications of structural control under earthquake excitations. In fact, the control of earthquake-excited structures presents a unique problem of its own in the area of active control. The main objective of this

report is to develop and propose new optimal control laws suitable for application to seismic-excited building structures.

A critical review of classical optimal control theories for applications to earthquake engineering problems is made. It is shown that the Riccati matrix represents the optimal closed-loop control only in the absence of continuous external excitations. In earthquake applications where the ground acceleration is the major source of continuous disturbances, the Riccati matrix does not satisfy the condition for optimal closed-loop control. It is shown that the optimal open-loop control and the optimal closed-open-loop control are superior to the closed-loop control using the Riccati matrix. Unfortunately, these two classical optimal control algorithms are not applicable to earthquake-excited structures. This is because for these optimal control algorithms to be applicable the entire earthquake ground acceleration history should be known a priori.

Although the entire earthquake base excitation history to the building is not known a priori, it can be measured real-time on-line by installing sensors on the basement floor. In other words, at any time t, the earthquake record is available up to that time instant t. Such measured information is used to develop new control laws. The objective function used for establishing new control laws is the time dependent performance index expressed in terms of quadratic functions. Since the time dependent performance index is minimized at every time instant, these newly developed optimal control algorithms are referred to as the instantaneous optimal control laws, including the instantaneous optimal closed-loop control, instantaneous optimal open-loop control and instantaneous optimal closed-open-loop control. Numerical examples are worked out to demonstrate the efficiency of these new control laws. Likewise, experimental verifications for these control laws have been conducted at SUNY, Buffalo [Ref. 47].

SECTION 2
CRITICAL REVIEW OF CLASSICAL OPTIMAL CONTROL
THEORIES FOR EARTHQUAKE-EXCITED STRUCTURES

In this chapter, various optimal control algorithms will be critically reviewed from the standpoint of applications to earthquake engineering problems. From such a review it will become apparent that there is a need to develop new optimal control algorithms suitable for controlling earthquake-excited structures.

For simplicity, consider a one-dimensional building structure implemented by an active tendon control system as shown in Fig. 2.1. The structure is idealized by an n degrees of freedom system and subjected to a one-dimensional earthquake ground acceleration $\ddot{X}_0(t)$. The matrix equation of motion can be expressed as

$$\dot{Z}(t) = A\ Z(t) + B\ U(t) + W_1 \ddot{X}_0(t) \tag{2.1}$$

with the initial condition $Z(0) = 0$. In Eq. (2.1), $Z(t)$ = 2n state vector, $U(t)$ = r dimensional control vector, A = 2nx2n matrix, B = a (2nxr) matrix specifying the locations of active controllers, and W_1 is an appropriate 2n vector [see Appendix A for these matrices]. In what follows, a prime denotes the transpose of a vector or matrix.

The standard quadratic performance index J is given in the following

$$J = \int_0^{t_f} [Z'(t)\ Q\ Z(t) + U'(t)\ R\ U(t)]dt \tag{2.2}$$

in which $\underset{\sim}{Q}$ is a (2nx2n) positive semi-definite matrix, $\underset{\sim}{R}$ is a (rxr) positive definite matrix, and t_f is a duration defined to be longer than that of the earthquake.

To minimize the performance index J subjected to the constraint given by Eq. (2.1), the necessary conditions can be shown as follows [e.g., Ref. 70 and Appendix B].

$$\dot{\underset{\sim}{\lambda}}(t) = - \underset{\sim}{A}' \; \underset{\sim}{\lambda}(t) - 2 \underset{\approx}{Q} \; \underset{\sim}{Z}(t) \quad ; \quad \underset{\sim}{\lambda}(t_f) = 0 \tag{2.3}$$

$$\underset{\sim}{U}(t) = - \tfrac{1}{2}\underset{\sim}{R}^{-1} \; \underset{\sim}{B}' \; \underset{\sim}{\lambda}(t) \tag{2.4}$$

in which $\underset{\sim}{\lambda}(t)$ is a 2n vector representing the costate variables (or Lagrangian multipliers). The optimal control vector $\underset{\sim}{U}(t)$, the costate vector $\underset{\sim}{\lambda}(t)$, and the state vector $\underset{\sim}{Z}(t)$ can be solved using Eqs. (2.1), (2.3), and (2.4). It follows from Eq. (2.4) that the control vector $\underset{\sim}{U}(t)$ is proportional to the costate vector $\underset{\sim}{\lambda}(t)$.

For the general case in which the control vector $\underset{\sim}{U}(t)$ (or the costate vector $\underset{\sim}{\lambda}(t)$) is regulated by the response state vector and the external excitation, one has

$$\underset{\sim}{\lambda}(t) = \underset{\sim}{P}(t) \; \underset{\sim}{Z}(t) + \underset{\sim}{q}(t) \quad ; \quad \underset{\sim}{\lambda}(t_f) = 0 \tag{2.5}$$

where the first term on the right-hand side indicates the closed-loop control and the second term represents the open-loop control.

The unknown matrix $\underset{\sim}{P}(t)$ and vector $\underset{\sim}{q}(t)$ can be determined by substituting Eq. (2.5) into Eqs. (2.1), (2.3) and (2.4) leading to the following expression

$$[\dot{\underset{\sim}{P}}(t) + \underset{\sim}{P}(t) \ \underset{\sim}{A} -$$

$$\tfrac{1}{2}\underset{\sim}{P}(t) \ \underset{\sim}{B} \ \underset{\sim}{R}^{-1} \ \underset{\sim}{B}' \ \underset{\sim}{P}(t) + \underset{\sim}{A}' \ \underset{\sim}{P}(t) + 2\underset{\sim}{Q}] \ \underset{\sim}{Z}(t)$$

$$+ \ \dot{\underset{\sim}{q}}(t) - [\tfrac{1}{2}\underset{\sim}{P}(t) \ \underset{\sim}{B} \ \underset{\sim}{R}^{-1} \ \underset{\sim}{B}' - \underset{\sim}{A}'] \ \underset{\sim}{q}(t)$$

$$+ \ \underset{\sim}{P}(t) \ \underset{\sim}{W}_1 \ddot{X}_0(t) = 0 \qquad\qquad (2.6)$$

2.1 Optimal Closed-Loop Control

For the special case in which the control force is regulated by the response state vector alone, i.e., $\underset{\sim}{q}(t) = 0$ in Eq. (2.5), one has

$$\underset{\sim}{\lambda}(t) = \underset{\sim}{P}(t) \ \underset{\sim}{Z}(t) \qquad\qquad (2.7)$$

Then Eq. (2.6) reduces to

$$[\dot{\underset{\sim}{P}}(t) + \underset{\sim}{P}(t) \ \underset{\sim}{A} - \tfrac{1}{2}\underset{\sim}{P}(t) \ \underset{\sim}{B} \ \underset{\sim}{R}^{-1} \ \underset{\sim}{B}' \ \underset{\sim}{P}(t) + \underset{\sim}{A}' \ \underset{\sim}{P}(t)$$

$$+ \ 2\underset{\sim}{Q}] \ \underset{\sim}{Z}(t) + \underset{\sim}{P}(t) \ \underset{\sim}{W}_1 \ddot{X}_0(t) = 0 \quad ;$$

$$\underset{\sim}{P}(t_f) = 0 \qquad\qquad (2.8)$$

When the earthquake ground acceleration $\ddot{X}_0(t)$ is zero, Eq. (2.8) becomes

$$[\dot{\underset{\sim}{P}}(t) + \underset{\sim}{P}(t) \ \underset{\sim}{A} - \tfrac{1}{2}\underset{\sim}{P}(t) \ \underset{\sim}{B} \ \underset{\sim}{R}^{-1} \ \underset{\sim}{B}' \ \underset{\sim}{P}(t) +$$

$$\underset{\sim}{A}' \ \underset{\sim}{P}(t) + 2\underset{\sim}{Q}] = 0 \quad ; \quad \underset{\sim}{P}(t_f) = 0 \qquad\qquad (2.9)$$

Equation (2.9) is the classical matrix Riccati equation and $\underset{\sim}{P}(t)$ is the Riccati matrix.

Strictly speaking, the Riccati matrix $\underset{\sim}{P}(t)$ obtained from Eq. (2.9) does not correspond to the optimal closed-loop control for the earthquake-excited building structure, because it is obtained by setting the ground acceleration $\ddot{X}_0(t)$ to zero. Hence, the optimal closed-loop control is achieved by the Riccati matrix only if the earthquake excitation is either zero or a white noise random process [e.g., Refs. 50, 70]. It is mentioned that the Riccati matrix, Eq. (2.9), depends exclusively on the structural characteristics and the weighting matrices $\underset{\sim}{Q}$ and $\underset{\sim}{R}$. For building structures, extensive experience indicates that the Riccati matrix $\underset{\sim}{P}(t)$ remains constant (i.e., each element of $\underset{\sim}{P}(t)$ remains constant) over the entire duration of earthquake excitation and it drops rapidly to zero near t_f. In other words, $\underset{\sim}{P}(t)$ establishes a stationary state in a very short period of time starting from t_f backwards. Typical elements of $\underset{\sim}{P}(t)$ for an eight story building are shown in Fig. 2.2. As a result, the effectiveness of the control system is not affected, when the Riccati matrix is approximated by a constant matrix, i.e., $\underset{\sim}{P}(t) = \underset{\sim}{P}$ or $\dot{\underset{\sim}{P}}(t) = 0$, as long as t_f is longer than the earthquake duration. Consequently, for building structures under earthquake excitations, the constant Riccati matrix $\underset{\sim}{P}$ can be used, and Eq. (2.9) becomes a matrix algebraic equation

$$\underset{\sim}{P}\ \underset{\sim}{A} - \tfrac{1}{2}\underset{\sim}{P}\ \underset{\sim}{B}\ \underset{\sim}{R}^{-1}\ \underset{\sim}{B}'\ \underset{\sim}{P} + \underset{\sim}{A}'\ \underset{\sim}{P} + 2\underset{\sim}{Q} = 0 \qquad (2.10)$$

It is emphasized that, in general, the optimal closed-loop control requires the measurements of the full state vector $\underset{\sim}{Z}(t)$, i.e., $2n$ sensors are needed. Such a complete measurement may not be possible for complex buildings.

2.2 Optimal Closed-Open-Loop Control

When the control vector $\underset{\sim}{U}(t)$ is expressed in the form of Eq. (2.4) and (2.5), the control law is referred to as the optimal

closed-open-loop control. In this case the control vector is
determined by the measured state vector and the earthquake ground
acceleration. The Riccati matrix $\underset{\sim}{P}$ and the vector $\underset{\sim}{q}(t)$ are
obtained from Eq. (2.6) as follows:

$$\underset{\sim}{P} \underset{\sim}{A} - \tfrac{1}{2} \underset{\sim}{P} \underset{\sim}{B} \underset{\sim}{R}^{-1} \underset{\sim}{B}' \underset{\sim}{P} + \underset{\sim}{A}' \underset{\sim}{P} + 2\underset{\sim}{Q} = 0 \qquad (2.11)$$

$$\underset{\sim}{\dot{q}}(t) - [\tfrac{1}{2}\underset{\sim}{P} \underset{\sim}{B} \underset{\sim}{R}^{-1} \underset{\sim}{B}' - \underset{\sim}{A}']\underset{\sim}{q}(t) + \underset{\sim}{P} \underset{\sim}{W}_1 \ddot{X}_0(t) = 0 \quad ;$$

$$\underset{\sim}{q}(t_f) = 0 \qquad (2.12)$$

in which the time dependent Riccati matrix $\underset{\sim}{P}(t)$ has been
approximated by a constant matrix $\underset{\sim}{P}$, i.e., $\underset{\sim}{P}(t) = \underset{\sim}{P}$. The
validity of such an approximation has been substantiated by
extensive numerical results [Ref. 58]

Unlike the Ricatti closed-loop control, in which the gain of the
control vector is obtained independent of (or disregard with) the
earthquake excitation, the optimal closed-open-loop control given
by Eqs. (2.11) and (2.12) utilizes the information of earthquake
excitations. Hence, it should be superior to the Riccati
closed-loop control.

Unfortunately, the optimal closed-open-loop control is not
achievable for the earthquake excitation. This is because $\underset{\sim}{q}(t)$
in Eq. (2.12) should be solved backwards from the terminal time
t_f, indicating that the entire earthquake history $\ddot{X}_0(t)$ should be
known a priori. Although the earthquake excitation $\ddot{X}_0(t)$ is
measurable, it is not known a priori.

The optimal closed-open-loop control is feasible only if Eq.
(2.12) can be solved forwards starting from t = 0. However, the
solution for $q(t)$ is always numerically unstable when solving
forwards from t = 0, because the real parts of the eigenvalues

are positive. For instance, given the entire excitation history $\ddot{X}_0(t)$ a priori, $\underset{\sim}{q}(t)$ and $\underset{\sim}{q}(0)$ can be solved backwards starting from t_f. Then, using the $\underset{\sim}{q}(0)$ obtained previously, it is difficult to reproduce $\underset{\sim}{q}(t)$ by solving Eq. (2.12) forwards because the resulting numerical solution for $\underset{\sim}{q}(t)$ is divergent [see Ref. 58 for detailed discussions].

2.3 Optimal Open-Loop Control

For the open-loop control, the control vector depends only on the earthquake excitation, i.e., independent of the response state vector $\underset{\sim}{Z}(t)$. Thus, Eq. (2.5) becomes

$$\underset{\sim}{\lambda}(t) = \underset{\sim}{q}(t) \tag{2.13}$$

and Eq. (2.6) reduces to

$$\dot{\underset{\sim}{q}}(t) = -\underset{\sim}{A}' \, \underset{\sim}{q}(t) - 2\underset{\sim}{Q} \, \underset{\sim}{Z}(t) \quad ; \quad \underset{\sim}{q}(t_f) = 0 \tag{2.14}$$

which is identical to Eq. (2.3). Substitution of Eqs. (2.4) and (2.13) into Eq. (2.1) leads to the following expression

$$\dot{\underset{\sim}{Z}}(t) = \underset{\sim}{A} \, \underset{\sim}{Z}(t) - \tfrac{1}{2} \underset{\sim}{B} \, \underset{\sim}{R}^{-1} \, \underset{\sim}{B}' \underset{\sim}{q}(t) + \underset{\sim}{W}_1 \ddot{X}_0(t)$$
$$; \quad \underset{\sim}{Z}(0) = 0 \tag{2.15}$$

The state vector $\underset{\sim}{Z}(t)$ and the vector $\underset{\sim}{q}(t)$ can be solved using Eqs. (2.14) and (2.15). Again, the optimal open-loop control cannot be implemented because $\underset{\sim}{q}(t)$ should be solved backwards from the terminal time t_f, and the earthquake excitation $\ddot{X}_0(t)$ should be known a priori.

2.4 Simulation of Earthquake Ground Acceleration $\ddot{X}_0(t)$

The earthquake ground acceleration, $\ddot{X}_0(t)$, is modeled as a uniformly modulated non-stationary random process;

$$\ddot{X}_0(t) = \psi(t)\ddot{X}(t) \tag{2.16}$$

in which, $\psi(t)$ is a deterministic non-negative envelope function and $\ddot{X}(t)$ is a stationary random process with zero mean and a power spectral density $\Phi_{\ddot{X}\ddot{X}}(\omega)$. A commonly used spectral density $\Phi_{\ddot{X}\ddot{X}}(\omega)$ for the stationary process $\ddot{X}(t)$ is considered,

$$\Phi_{\ddot{X}\ddot{X}}(\omega) = \frac{1 + 4\zeta_g^2(\omega/\omega_g)^2}{[1 - (\omega/\omega_g)^2]^2 + 4\zeta_g^2(\omega/\omega_g)^2} \cdot s^2 \tag{2.17}$$

in which ζ_g, ω_g and S are parameters depending on the intensity and the characteristics of the earthquake in a particular geological location.

Various types of envelope function $\psi(t)$ have been used in the literature. A particular envelope function given in the following will be used

$$\psi(t) = \begin{cases} 0 & ; & t < 0 \\ (t/t_1)^2 & ; & 0 \leq t \leq t_1 \\ 1 & ; & t_1 \leq t \leq t_2 \\ \exp[-c(t-t_2)] & ; & t > t_2 \end{cases} \tag{2.18}$$

where t_1, t_2 and c are parameters which should be selected appropriately to reflect the shape and duration of the earthquake ground acceleration.

Physically, $\psi(t)$ describes the amplitude modulation whereas the spectral density $\Phi_{\ddot{X}\ddot{X}}(\omega)$ specifies the frequency content of the earthquake ground acceleration $\ddot{X}_0(t)$. Furthermore, since the ground acceleration has a zero mean, the mean values of the response vector and the active control force are all zero.

The non-stationary earthquake ground acceleration $\ddot{X}_0(t)$ given by Eq. (2.16) can be simulated conveniently using the Fast Fourier Transform (FFT) technique as follows [Refs. 41, 58, 71]:

$$\ddot{X}_0(t) = \psi(t)\sqrt{2\Delta\omega} \; \text{Re} \left\{ \sum_{k=1}^{M} \left[\sqrt{2\Phi_{\ddot{X}\ddot{X}}(\omega_k)} \; e^{i\varphi_k} \right] e^{i\omega_k t} \right\} \qquad (2.19)$$

in which $\psi(t)$ is the deterministic non-negative envelope function given by Eq. (2.18), $\Phi_{\ddot{X}\ddot{X}}(\omega)$ is the power spectral density of $X(t)$ given by Eq. (2.17), and φ_k (k=1,2,...,M) are statistically independent and identically distributed random variables with the uniform distribution in $[0,2\pi,]$, i.e.,

$$\begin{cases} f_{\varphi_k}(x) = \dfrac{1}{2\pi} & \text{for } 0 \le x \le 2\pi \\[2mm] \quad\quad\;\; = 0 & \text{elsewhere} \end{cases}$$

where $f_{\varphi_k}(x)$ is the probability density function of the random variable φ_k (k=1,2,...M). In Eq. (2.19) the one-sided spectral density $2\Phi_{\ddot{X}\ddot{X}}(\omega)$ for $\omega \ge 0$ is evaluated at an equally spaced interval $\Delta\omega$ with $\omega_k = k\Delta\omega > 0$, and Re{ } represents the real part of the quantity in the bracket. In applying the FFT technique to Eq. (2.19), the earthquake ground acceleration $\ddot{X}_0(t)$ is also evaluated at equally spaced discrete points $\ddot{X}_0(t_j)$ with $t_j = j\Delta t$, j=1,2,...M. The total number of sample points M must be an integer power of 2 based on FFT algorithm.

2.5 Numerical Example

In order to compare the control efficiency for each control law, described above, it is assumed that the earthquake sample functions are known a priori. While such a hypothetical situation does not exist, the results will provide information regarding the effectiveness of the Riccati closed-loop control.

An eight-story building in which every story unit is identically constructed is considered for illustrative purpose. The structural properties of each story are: m = floor mass = 345.6 tons; k = elastic stiffness of each story unit = 3.404×10^5 KN/m; and c = internal damping coefficient of each story unit = 2,937 tons/sec that corresponds to a 2% damping for the first vibrational mode of the entire building. The external damping is assumed to be zero. The computed natural frequencies are 5.79, 17.18, 27.98, 37.82, 46.38, 53.36, 58.53, and 61.69 rad/sec. The parameter values associated with the earthquake ground acceleration model are as follows: t_1 = 3 sec, t_2 = 13 sec, c = 0.26 sec^{-1}, ζ_g = 0.65, ω_g = 18.85 rad/sec, and s^2 = 4.5×10^{-4} m^2/sec^2.

Active tendon controllers are installed in every story unit and the angle of inclination of the tendons with respect to the floor is 25°, see Fig. 2.1. Thus, the control force vector from the controllers is $\underset{\sim}{U}(t)/\cos 25°$. In the present situation, the dimensions of the weighting matrices $\underset{\sim}{Q}$ and $\underset{\sim}{R}$ are (16x16) and (8x8), respectively. For simplicity, both $\underset{\sim}{Q}$ and $\underset{\sim}{R}$ matrices are chosen to be diagonal matrices with elements Q_{11} = Q_{22} = $\ldots$ = Q_{88} = Q^* = 10^5, Q_{99} = $\ldots$ = $Q_{16,16}$ = 0, and R_{11} = R_{22} = $\ldots$ = R_{88} = R^* = 10^{-4}.

With the structure and weighting matrices given above, elements of Riccati matrix $\underset{\sim}{P}$ have been computed and some elements are

presented in Fig. 2.2. It is observed that these elements remain constant until reaching the terminal time t_f = 30 sec. In other words, the elements of Riccati matrix establish stationary values in a short period of time from t_f.

A sample function of the earthquake ground acceleration $\ddot{X}_0(t)$ has been simulated and shown in Fig. 2.3. With such an earthquake input, the structural response vector $\underline{Z}(t)$ has been computed. The results for the relative displacement of the top floor and the base shear force without active control are displayed in Figs. 2.4(a) and 2.5(a), respectively. The corresponding results obtained using the optimal open-loop and optimal closed-open-loop control algorithms are presented, respectively, in Figs. 2.4 and 2.5 as (b) and (c). Under these two control algorithms, the required active control force from the controller installed in the lowest story unit, referred to as the first controller, are shown in Figs. 2.6(a) and 2.6(b). With the Riccati closed-loop control, the results are displayed in Figs. 2.4(e), 2.5(e) and 2.6(c). Furthermore, the sub-optimal closed-loop control algorithm suggested in Refs. 39-41 has also been applied and the results are depicted in Figs. 2.4(d), 2.5(d) and 2.6(d).

The following observations are made based on Figs. 2.4-2.6.

(i)   With the application of active control systems, the building response quantities are reduced significantly.

(ii)   Under both the optimal open-loop control and optimal closed-open-loop control, the corresponding building responses and the required active control force are identical. This has been expected because both optimal control algorithms minimize the same objective function J.

(iii)   The control efficiency associated with the

2-10

optimal open-loop and closed-open-loop
control algorithms is better than that of the
Riccati closed-loop control. In other words,
the Riccati closed-loop control results
in higher response levels and larger
active control forces.

(iv) The control efficiency for the Riccati
closed-loop control is slightly better than
that of the sub-optimal closed-loop control.

When the earthquake ground acceleration $\ddot{X}_0(t)$ is considered as a
non-stationary random process with zero mean, the building
response quantities and the required active control forces are
all non-stationary random processes with zero mean. Then, the
usual spectral analysis of random vibration can be used to
determine the statistics of the building response as presented in
Appendix B. The time-dependent standard deviation (or root mean
square) of the top floor relative displacement, base shear force,
and required active control force from the first controller are
presented in Figs. 2.7(a), (b), and (c), respectively, when the
optimal closed-open-loop control algorithm is employed. In these
figures, the solid curve represents the response quantities
without active control. The dotted curve and dash-dotted curve
denote the results using active control system in which all
elements of the weighting matrix $\underset{\sim}{R}$ are equal to 10^{-3} and 10^{-4},
respectively. The corresponding results based on different
control algorithms are presented in Figs. 2.8-2.10.

From Figs. 2.7-2.10, the maximum root mean squares (or the
maximum standard deviations) of (i) the top floor relative
displacement, $\sigma_m(Y_8) = \text{maxi } \sigma(Y_8,t)$, (ii) the based shear force,
$\sigma_m(kY_1) = \text{maxi } \sigma(kY_1,t)$ and (iii) the active control force,
$\sigma_m(U_1)$, from the first controller, are summarized in Table 2.1
for different control algorithms. In Table 2.1, the maximum
response quantities, $\sigma_m(Y_8)$ and $\sigma_m(kY_1)$, have been normalized

2-11

with respect to the corresponding uncontrolled ones, $\sigma_m^*(Y_8)$ and $\sigma_m^*(kY_1)$, respectively.

It is observed from Figs. 2.7-2.10 and Table 2.1 that the Riccati closed-loop control is definitely inferior to both the optimal closed-open-loop control and optimal open-loop control. The sub-optimal closed-loop control is as efficient as the Riccati closed-loop control. As expected, the structural response quantities reduce and the required active control forces increase as the elements of the weighting matrix $\underset{\sim}{R}$ decreases.

TABLE 2-1 Maximum Root Mean Square of Non-Stationary Structural Response Quantities and Control Force; For 8-Story Building; Global Control

$$\sigma_m^*(Y_8) = 1.663 \text{ CM} \qquad \sigma_m^*(KY_1) = 1,116 \text{ KN}$$

CONTROL LAW	R^*	$\dfrac{\sigma_m(Y_8)}{\sigma_m^*(Y_8)}$	$\dfrac{\sigma_m(KY_1)}{\sigma_m^*(KY_1)}$	$\sigma_m(U_1)$ KN
Optimal Open-Loop Control	10^{-4} 10^{-3}	0.164 0.363	0.163 0.363	95 49
Optimal Closed-Open- Loop Control	10^{-4} 10^{-3}	0.164 0.363	0.162 0.362	95 49
Riccati Closed-Loop Control	10^{-4} 10^{-3}	0.309 0.558	0.313 0.557	170 75
Sub-Optimal Closed- Loop Control	Control Parameters $\epsilon=10,\tau=10$ $\epsilon=10,\tau=3$	0.313 0.519	0.372 0.528	181 88
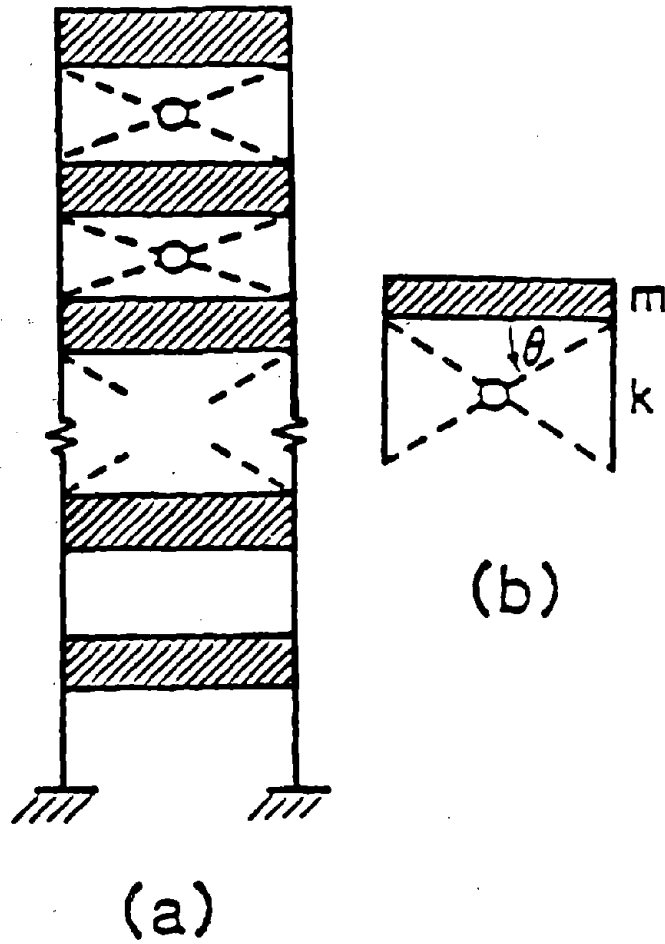
FIGURE 2-1   Structural Model of a Multi-Story Building With Active Control
System; (a) Active Tendon System, (b) Story Unit.
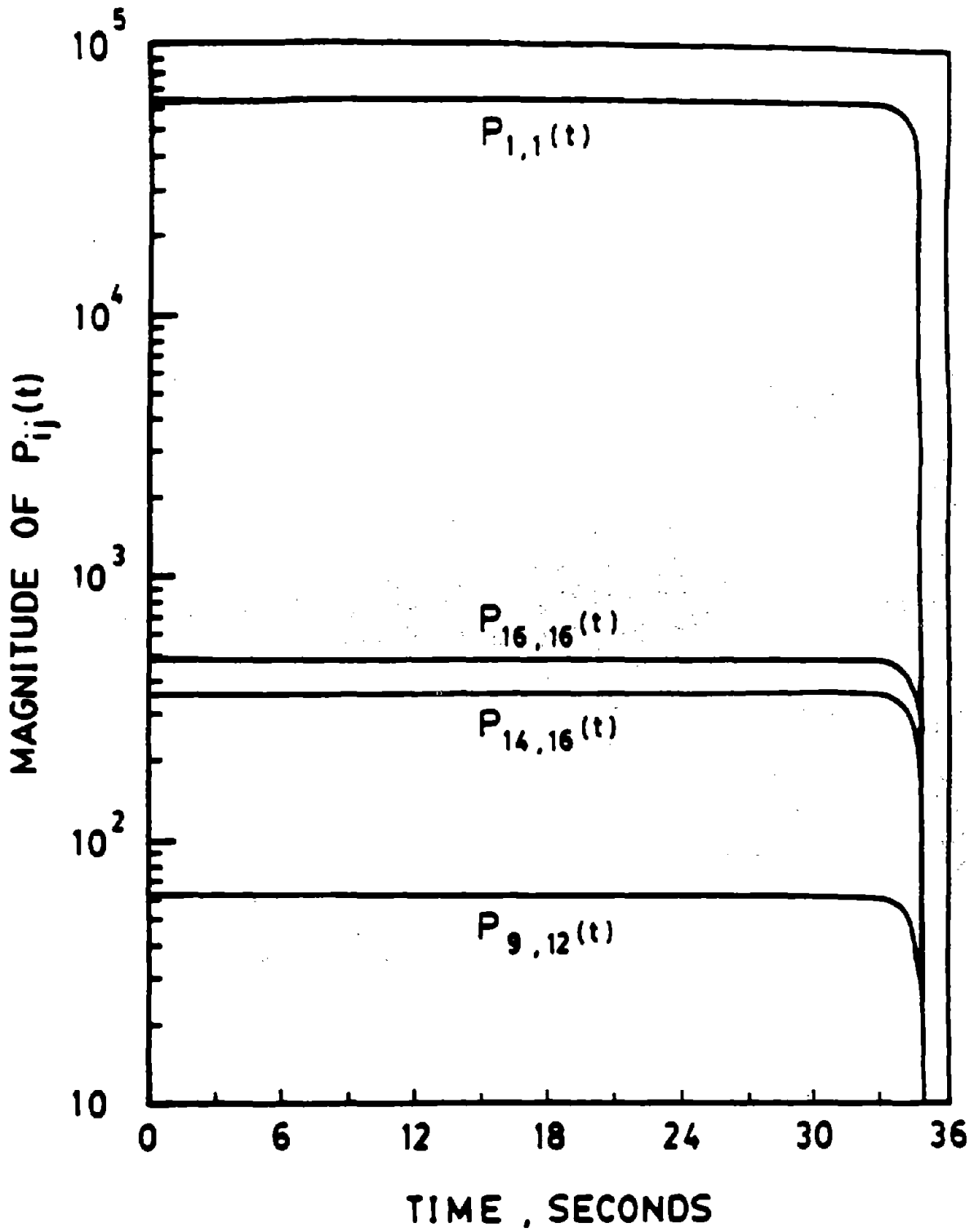
FIGURE 2-2   Some Elements of Riccati Matrix, P(t).
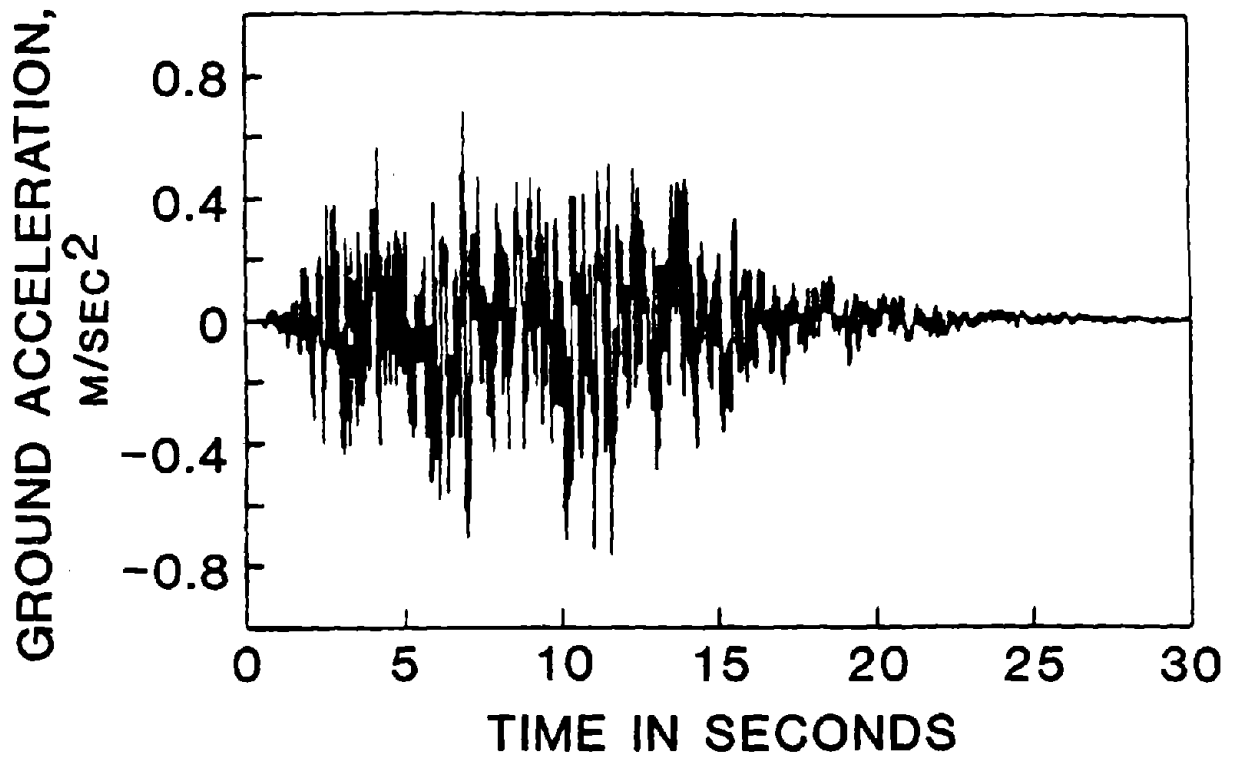
FIGURE 2-3   Simulated Ground Acceleration
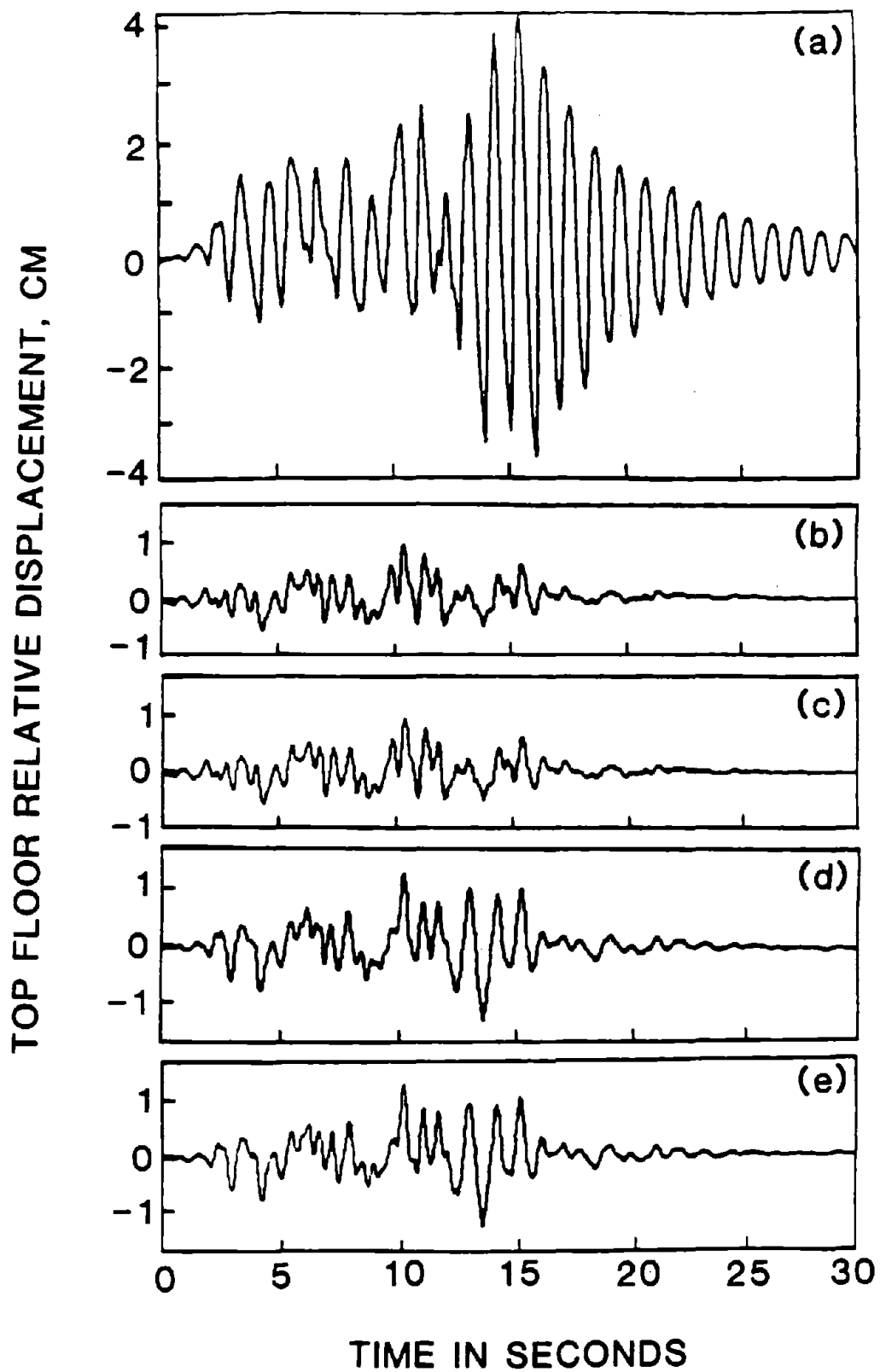
FIGURE 2-4   Top Floor Relative Displacement: (a) No Control; (b) Optimal Open-Loop Control; (c) Optimal Closed-Open-Loop Control; (d) Sub-Optimal Closed-Loop Control; (e) Riccati Closed-Loop Control.

2-17
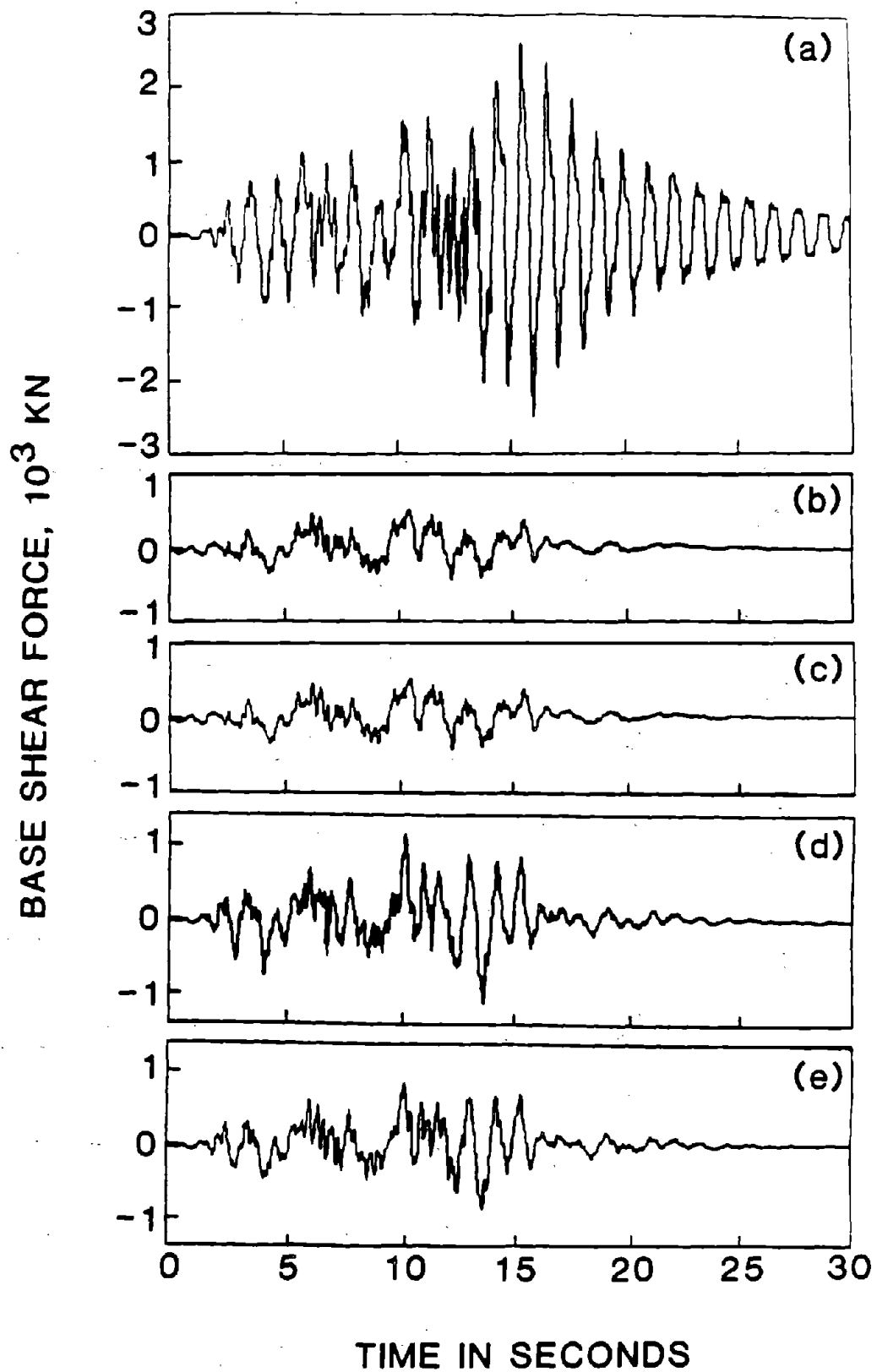
FIGURE 2-5 Base Shear Force: (a) No Control; (b) Optimal Open-Loop
Control; (c) Optimal Closed-Open-Loop Control; (d) Sub-Optimal
Closed-Loop Control; (e) Riccati Closed-Loop Control.
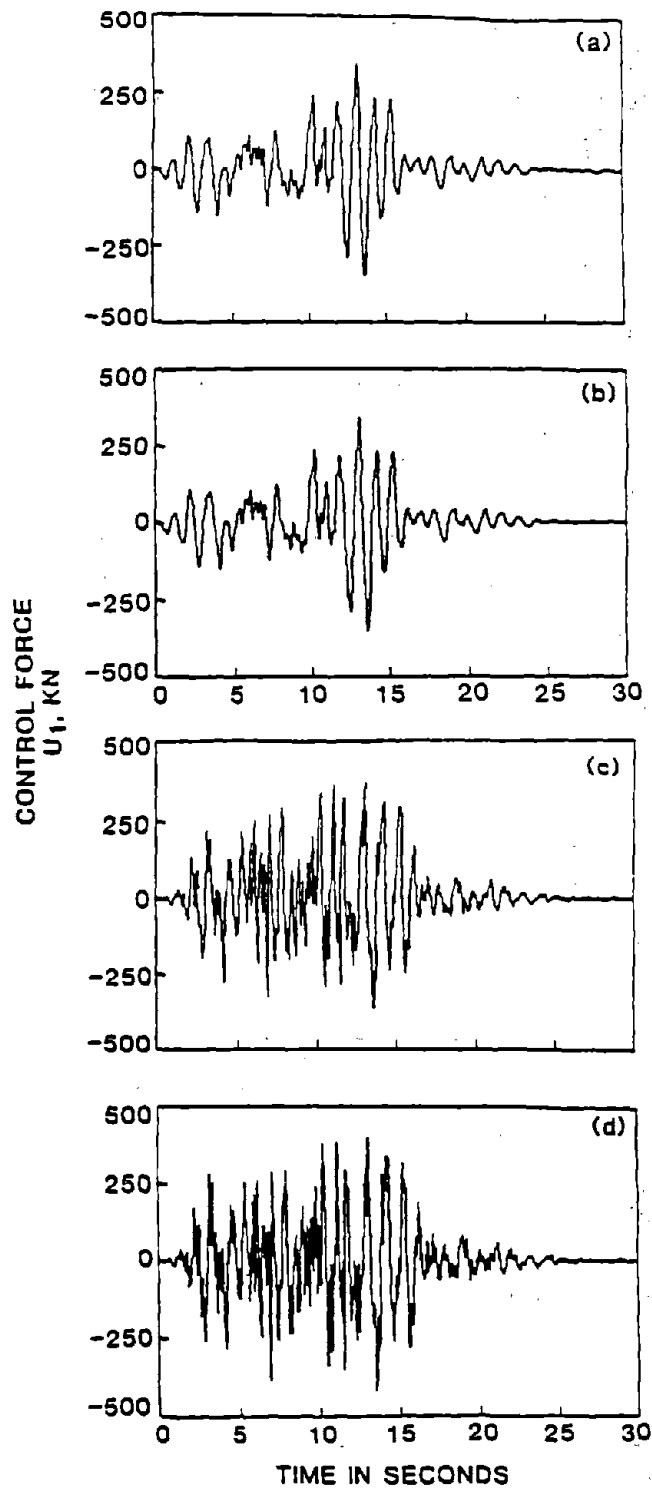
FIGURE 2-6   Control Force From First Controller: (a) Optimal
              Closed-Open-Loop Control; (b) Optimal Open-Loop Control; (c)
              Riccati Closed-Loop Control; (d) Sub-Optimal Closed-Loop
              Control.

2-19
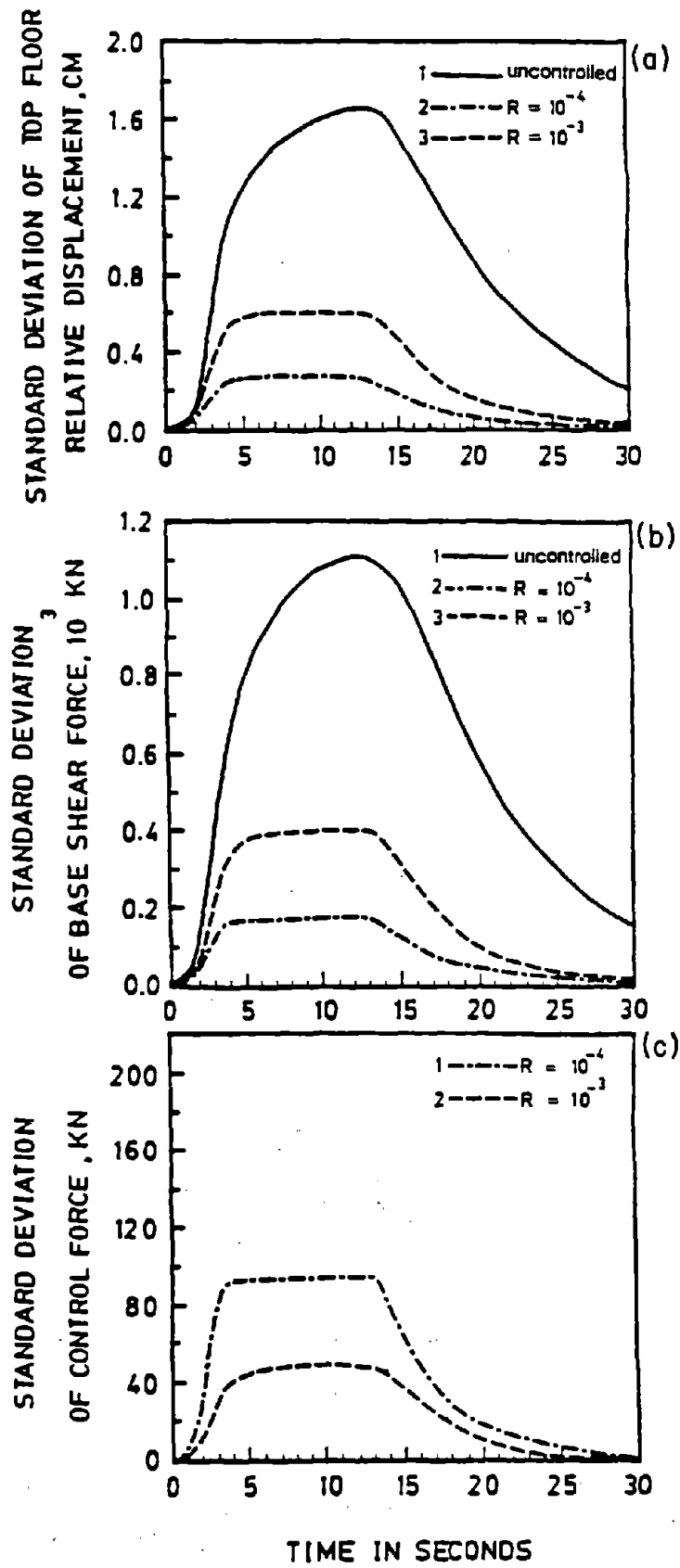
FIGURE 2-7 Optimal Closed-Open-Loop Control, (a) Standard Deviation of Top Floor Relative Displacement; (b) Standard Deviation of Base Shear Force; (c) Standard Deviation of Control Force From the First Controller.

2-20
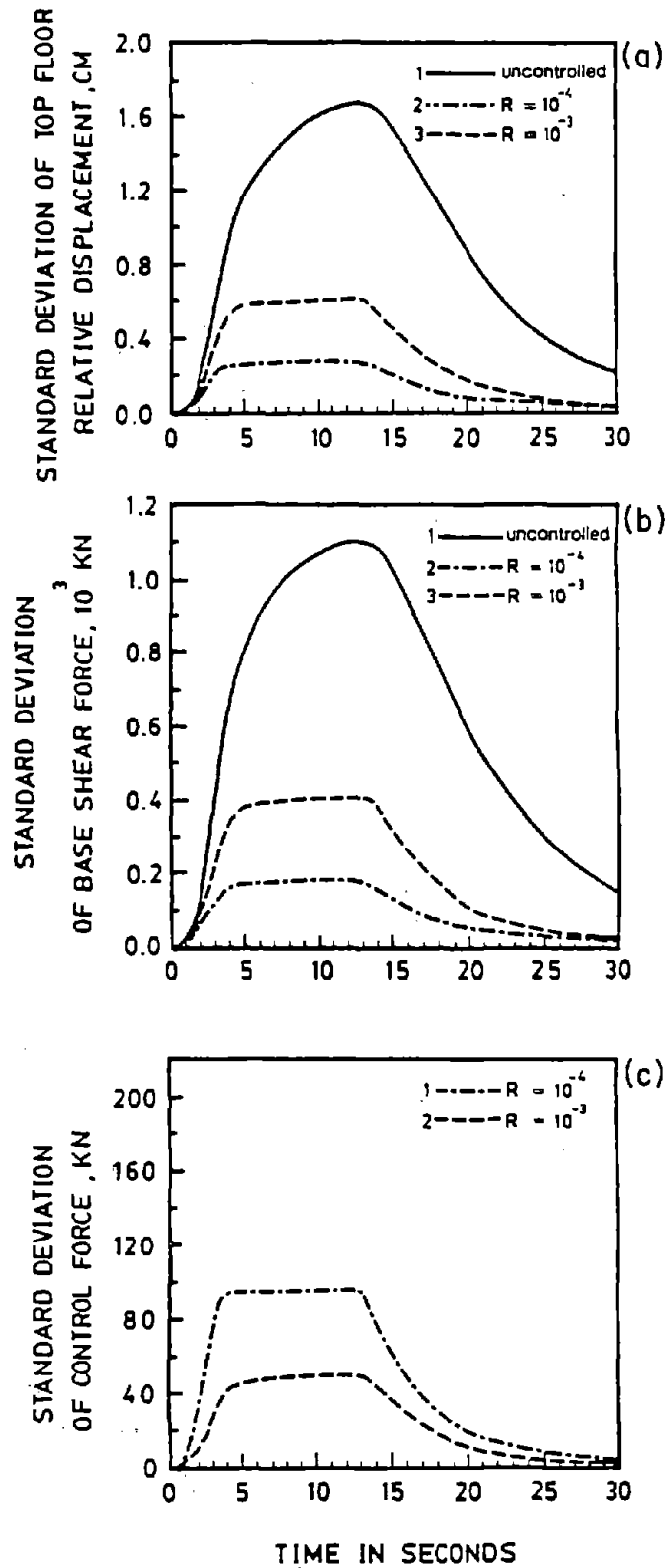
FIGURE 2-8   Optimal Open-Loop Control, (a) Standard Deviation of Top Floor
Relative Displacement; (b) Standard Deviation of Base Shear
Force; (c) Standard Deviation of Control Force From the First
Controller.
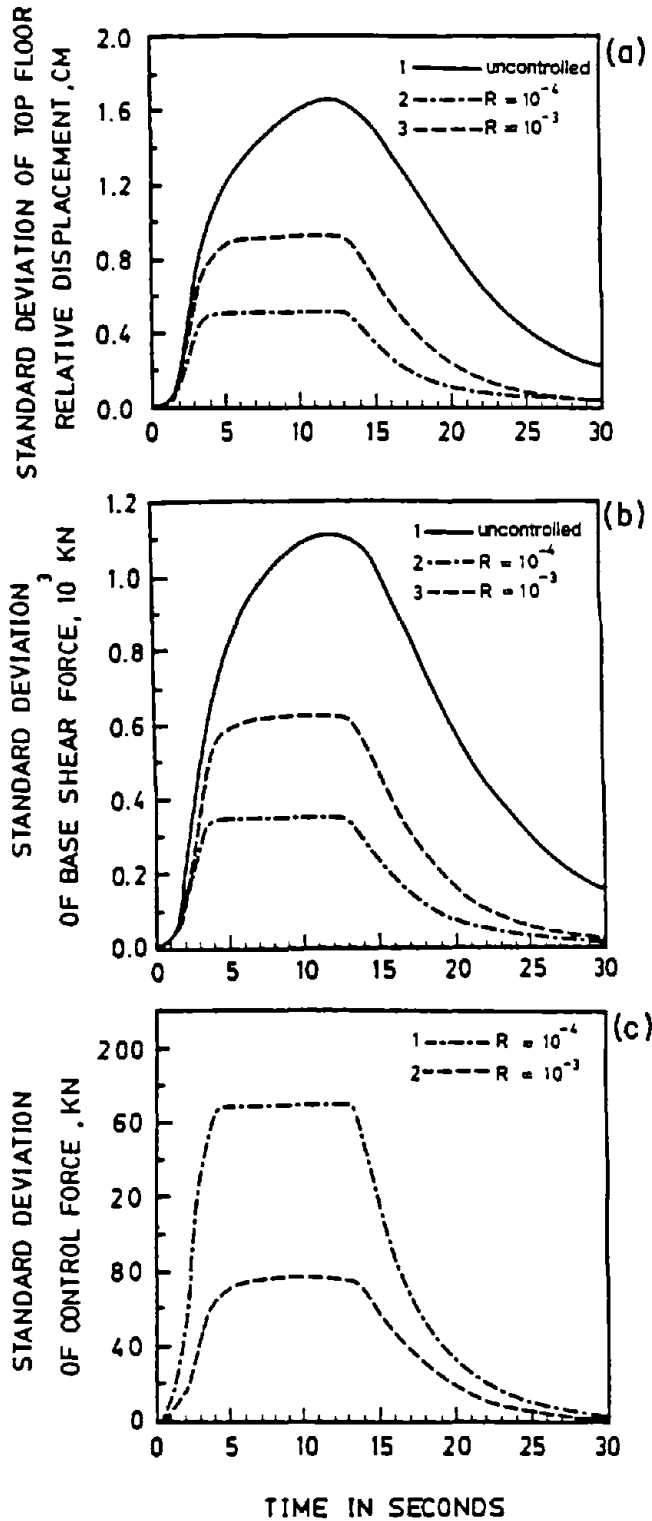
FIGURE 2-9   Riccati Closed-Loop Control, (a) Standard Deviation of Top Floor
Relative Displacement; (b) Standard Deviation of Base Shear
Force; (c) Standard Deviation of Control Force From the First
Controller.

2-22
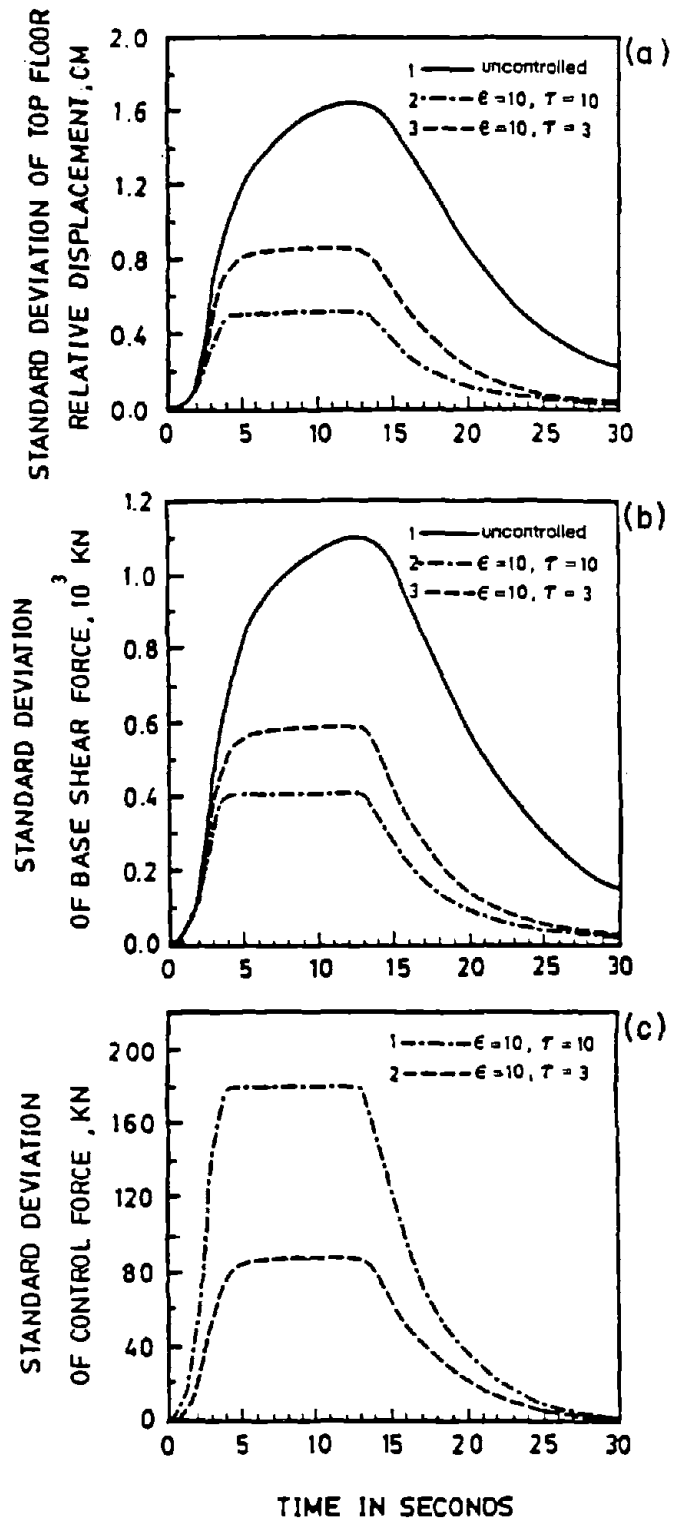
FIGURE 2-10   Sub-Optimal Closed-Loop Control (a) Standard Deviation of Top
Floor Relative Displacement; (b) Standard Deviation of Base
Shear Force; Standard Deviation of Control Force From the First
Controller.

SECTION 3
DEVELOPMENT OF NEW OPTIMAL
CONTROL ALGORITHMS FOR APPLICATIONS
TO EARTHQUAKE ENGINEERING PROBLEMS

It is obvious from the previous chapter that under seismic loads, the Riccati closed-loop control law does not satisfy the optimal condition, whereas the optimal open-loop control and optimal closed-open-loop control algorithms are not applicable, because the earthquake ground motion is not known a priori. While the earthquake ground motion is not known a priori, the base excitation of the building can be measured real-time on-line by installing sensors on the basement floor. In other words, at any particular time t, the base excitation record is available up to that time instant t. Such important information will be utilized in the development of new optimal control algorithms in this chapter.

The reason why it is not feasible to apply the classical optimal open-loop or closed-open-loop control algorithm to earthquake-excited structures stems from the definition of the performance index J. The performance index J given by Eq. (2.2) is the integral of quadratic functions over the time interval $(0, t_f)$. In order to minimize the quantity J defined over the time interval $(0, t_f)$, the input excitation in that time interval should be known a priori. Consequently, new optimal control algorithms will be established using the time dependent performance index J(t) as follows

$$J(t) = \underset{\sim}{Z}'(t) \underset{\sim}{Q} \underset{\sim}{Z}(t) + \underset{\sim}{U}'(t) \underset{\sim}{R} \underset{\sim}{U}(t) \tag{3.1}$$

The implication of minimizing Eq. (3.1) is that the performance index J(t) is minimized at every time instant t for all $0 \leq t \leq t_f$. Hence, the optimal control law thus obtained is referred to as the instantaneous optimal control law.

3.1 Development of Instantaneous Optimal Control Algorithms

The system of equations of motion given in Eq. (2.1) can be decoupled through the following transformation:

$$\underset{\sim}{Z}(t) = \underset{\sim}{T}\,\underset{\sim}{Y}_1(t) \qquad\qquad (3.2)$$

in which $\underset{\sim}{T}$ is a (2nx2n) modal matrix consisting of eigenvectors of $\underset{\sim}{A}$.

Substituting Eq. (3.2) into Eq. (2.1), one obtains the decoupled equations of motion as follows:

$$\dot{\underset{\sim}{Y}}_1(t) = \underset{\sim}{\Theta}\,\underset{\sim}{Y}_1(t) + \underset{\sim}{F}(t) \qquad ; \qquad \underset{\sim}{Y}_1(0) = 0 \qquad\qquad (3.3)$$

in which $\underset{\sim}{\Theta}$ is a (2nx2n) diagonal matrix consisting of complex eigenvalues $\underset{\sim}{\Theta}_j$ (j=1,2,...,2n) of matrix $\underset{\sim}{A}$ and

$$\underset{\sim}{F}(t) = \underset{\sim}{T}^{-1}\,[\underset{\sim}{B}\,\underset{\sim}{U}(t) + \underset{\sim}{W}_1\ddot{\underset{\sim}{X}}_0(t)] \qquad\qquad (3.4)$$

The solution of Eq. (3.3) can be written as

$$\underset{\sim}{Y}_1(t) = \int_0^t \exp[\underset{\sim}{\Theta}(t-\tau)]\,\underset{\sim}{F}(\tau)\,d\tau \qquad\qquad (3.5)$$

where $\exp[\underset{\sim}{\Theta}(t-\tau)]$ is a (2nx2n) diagonal matrix with the jth diagonal element being $\exp[\Theta_j(t-\tau)]$.

The solution for the response vector given by Eq. (3.5) can be obtained as follows

$$\underset{\sim}{Y}_1(t) = \int_0^{t-\Delta t} \exp[\underset{\sim}{\Theta}(t-\tau)]\underset{\sim}{F}(\tau)d\tau$$

$$+ \int_{t-\Delta t}^{t} \exp[\underset{\sim}{\Theta}(t-\tau)] \underset{\sim}{F}(\tau) d\tau$$

$$= e^{\underset{\sim}{\Theta}\Delta t} \underset{\sim}{Y}_1(t-\Delta t)$$

$$+ \int_{t-\Delta t}^{t} \exp[\underset{\sim}{\Theta}(t-\tau)] \underset{\sim}{F}(\tau) d\tau \qquad (3.6)$$

$$\equiv e^{\underset{\sim}{\Theta}\Delta t} \underset{\sim}{Y}_1(t-\Delta t) + \frac{\Delta t}{2} [e^{\underset{\sim}{\Theta}\Delta t} \underset{\sim}{F}(t-\Delta t) + \underset{\sim}{F}(t)]$$

in which $e^{\underset{\sim}{\Theta}\Delta t}$ is a diagonal matrix with the jth diagonal element being $\exp[\Theta_j \Delta t]$.

Substitution of Eq. (3.6) into Eq. (3.2) leads to the following expression for the state vector

$$\underset{\sim}{Z}(t) = \underset{\sim}{T} e^{\underset{\sim}{\Theta}\Delta t} \underset{\sim}{Y}_1(t-\Delta t)$$

$$+ \frac{\Delta t}{2} \underset{\sim}{T}[e^{\underset{\sim}{\Theta}\Delta t} \underset{\sim}{F}(t-\Delta t) + \underset{\sim}{F}(t)]$$

$$= \underset{\sim}{T} e^{\underset{\sim}{\Theta}\Delta t} \underset{\sim}{T}^{-1} \underset{\sim}{Z}(t-\Delta t) +$$

$$\frac{\Delta t}{2} \underset{\sim}{T}[e^{\underset{\sim}{\Theta}\Delta t} \underset{\sim}{F}(t-\Delta t) + \underset{\sim}{F}(t)] \qquad (3.7)$$

in which $\underset{\sim}{F}(t)$ is given by Eq. (3.4) and $\underset{\sim}{F}(t-\Delta t)$ is obtained from Eq. (3.4) by replacing t by t-Δt. Substituting Eq. (3.4) into Eq. (3.7), one obtains

$$\underset{\sim}{Z}(t) = \underset{\sim}{T} \underset{\sim}{D}(t-\Delta t) + \frac{\Delta t}{2} [\underset{\sim}{B} \underset{\sim}{U}(t) + \underset{\sim}{W}_1 \ddot{X}_0(t)] \qquad (3.8)$$

in which

$$\underset{\sim}{D}(t-\Delta t) = e^{\underset{\sim}{\Theta}\Delta t}\underset{\sim}{T}^{-1}\Big\{\underset{\sim}{Z}(t-\Delta t) +$$

$$\frac{\Delta t}{2} [\underset{\sim}{B}\ \underset{\sim}{U}(t-\Delta t) + \underset{\sim}{W}_1\underset{\sim}{\ddot{X}}_0(t-\Delta t)]\Big\} \qquad (3.9)$$

is a vector containing all elements at t-Δt.

To minimize the performance index $J(t)$ given by Eq. (3.1) subjected to the constraint in Eq. (3.8), the Hamiltonian H is obtained in a similar manner as shown in Appendix B as follows

$$\underset{\sim}{H} = \underset{\sim}{Z}'(t)\underset{\approx}{Q}\ \underset{\sim}{Z}(t) + \underset{\sim}{U}'(t)\ \underset{\sim}{R}\ \underset{\sim}{U}(t) + \underset{\sim}{\lambda}'\{\underset{\sim}{Z}(t) -$$

$$\underset{\sim}{T}\ \underset{\sim}{D}(t-\Delta t) - \frac{\Delta t}{2} [\underset{\sim}{B}\ \underset{\sim}{U}(t) + \underset{\sim}{W}_1\underset{\sim}{\ddot{X}}_0(t)]\} \qquad (3.10)$$

where $\underset{\sim}{\lambda}$ is the costate vector or the Lagrangian multiplier vector.

The necessary conditions for minimizing the performance index $J(t)$ subjected to the constraint of the equations of motion are obtained in a similar manner as that shown in Appendix B.

$$\frac{\partial H}{\partial \underset{\sim}{Z}} = 0 \quad , \quad \frac{\partial H}{\partial \underset{\sim}{U}} = 0 \quad , \quad \frac{\partial H}{\partial \underset{\sim}{\lambda}} = 0 \qquad (3.11)$$

Upon substituting Eq. (3.10) into Eq. (3.11), one obtains

$$2\ \underset{\approx}{Q}\ \underset{\sim}{Z}(t) + \underset{\sim}{\lambda}(t) = 0 \qquad (3.12)$$

$$2\ \underset{\sim}{R}\ \underset{\sim}{U}(t) - \frac{\Delta t}{2}\ \underset{\sim}{B}'\ \underset{\sim}{\lambda}(t) = 0 \qquad (3.13)$$

$$\underset{\sim}{Z}(t) = \underset{\sim}{T}\ \underset{\sim}{D}(t-\Delta t) +$$

$$\frac{\Delta t}{2} [\underset{\sim}{B} \underset{\sim}{U}(t) + \underset{\sim}{W}_1 \ddot{X}_0(t)]$$ (3.14)

3.2 Instantaneous Optimal Open-Loop Control

The main advantage of the open-loop control for earthquake-excited structures lies in the fact that sensors are needed on the basement floor only. Since the measurement of the building response quantities are not necessary, the control system is simplified tremendously.

From Eq. (3.13), the control vector $\underset{\sim}{U}(t)$ is linearly proportional to the costate vector $\underset{\sim}{\lambda}(t)$. Let the control vector $\underset{\sim}{U}(t)$ be regulated by the earthquake excitation alone, i.e.,

$$\underset{\sim}{\lambda}(t) = \underset{\sim}{q}(t)$$ (3.15)

Then, Eqs. (3.12)-(3.14) become

$$2 \underset{\sim}{Q} \underset{\sim}{Z}(t) + \underset{\sim}{q}(t) = 0$$ (3.16)

$$2 \underset{\sim}{R} \underset{\sim}{U}(t) - \frac{\Delta t}{2} \underset{\sim}{B}' \underset{\sim}{q}(t) = 0$$ (3.17)

$$\underset{\sim}{Z}(t) = \underset{\sim}{T} \underset{\sim}{D}(t-\Delta t)$$

$$+ \frac{\Delta t}{2} [\underset{\sim}{B} \underset{\sim}{U}(t) + \underset{\sim}{W}_1 \ddot{X}_0(t)]$$ (3.18)

The unknown vectors $\underset{\sim}{U}(t)$, $\underset{\sim}{q}(t)$, and $\underset{\sim}{Z}(t)$ can be solved from Eqs. (3.16)-(3.18) as follows. The vector $\underset{\sim}{Z}(t)$ is eliminated by substituting Eq. (3.18) into Eq. (3.16) yielding

$$2 \underset{\sim}{Q} \left\{ \underset{\sim}{T} \underset{\sim}{D}(t-\Delta t) + \frac{\Delta t}{2} \left[\underset{\sim}{B} \underset{\sim}{U}(t) \right. \right.$$

$$\left. \left. + \underset{\sim}{W}_1 \ddot{X}_0(t) \right] \right\} + \underset{\sim}{g}(t) = 0 \tag{3.19}$$

Premultiplying Eq. (3.19) by $\frac{\Delta t}{2} \underset{\sim}{B}'$ and adding to Eq. (3.17), one obtains the control vector $\underset{\sim}{U}(t)$ in the following

$$\underset{\sim}{U}(t) = \underset{\sim}{L} \underset{\sim}{G}(t) \tag{3.20}$$

in which

$$\underset{\sim}{L} = [(\Delta t/2)^2 \underset{\sim}{B}' \underset{\sim}{Q} \underset{\sim}{B} + \underset{\sim}{R}]^{-1} \tag{3.21}$$

$$\underset{\sim}{G}(t) = - \frac{\Delta t}{2} \underset{\sim}{B}' \underset{\sim}{Q} \underset{\sim}{T} \underset{\sim}{D}(t-\Delta t) -$$

$$(\Delta t/2)^2 \underset{\sim}{B}' \underset{\sim}{Q} \underset{\sim}{W}_1 \ddot{X}_0(t) \tag{3.22}$$

where $\underset{\sim}{D}(t-\Delta t)$ is a vector consisting of all elements defined at $(t-\Delta t)$, see Eq. (3.9).

It is observed from Eqs. (3.20)-(3.22) that the control vector $\underset{\sim}{U}(t)$ at time t is regulated by the earthquake excitation $\ddot{X}_0(t)$ at time t and $\underset{\sim}{D}(t-\Delta t)$, that consists of earthquake excitation $\ddot{X}_0$ $(t-\Delta t)$, the control vector $\underset{\sim}{U}(t-\Delta t)$ and the response vector $\underset{\sim}{Z}(t-\Delta t)$ all at $t-\Delta t$, see Eq. (3.9). The response state vector $\underset{\sim}{Z}(t)$ under the instantaneous optimal open-loop control is obtained by substituting Eq. (3.20) into Eq. (3.18),

$$\underset{\sim}{Z}(t) = \underset{\sim}{T} \underset{\sim}{D}(t-\Delta t)$$

$$+ \frac{\Delta t}{2} \underset{\sim}{B} \underset{\sim}{L} \underset{\sim}{G}(t) + \frac{\Delta t}{2} \underset{\sim}{W}_1 \ddot{X}_0(t) \tag{3.23}$$

3.3 Instantaneous Optimal Closed-Loop Control

Let the control vector $U(t)$ (or the costate vector $\lambda(t)$) be regulated by the feedback response state vector $Z(t)$ alone, i.e.,

$$\lambda(t) = \Lambda\, Z(t) \tag{3.24}$$

Then, substitution of Eq. (3.24) into Eq. (3.12) yields

$$(2\, Q + \Lambda)\, Z(t) = 0 \tag{3.25}$$

from which the unknown matrix Λ is obtained, for $Z(t) \neq 0$, as

$$\Lambda = -2\, Q \tag{3.26}$$

The control vector $U(t)$ under the instantaneous optimal closed-loop control is obtained by substituting Eq. (3.26) into Eq. (3.24) and then into Eq. (3.13) as follows

$$U(t) = -\frac{\Delta t}{2}\, R^{-1}\, B'\, Q\, Z(t) \tag{3.27}$$

The response state vector $Z(t)$ under the optimal closed-loop control is determined from Eq. (3.14) with the aid of Eq. (3.27) as follows

$$Z(t) = [I + (\Delta t/2)^2 B\, R^{-1} B' Q]^{-1} [T\, D(t-\Delta t)$$
$$+ \frac{\Delta t}{2}\, W_1 \ddot{X}_0(t)] \tag{3.28}$$

in which I is an (2nx2n) identity matrix.

3.4 Instantaneous Optimal Closed-Open-Loop Control

Let the control vector $U(t)$ or $\lambda(t)$ be regulated by both the feedback response state vector $Z(t)$ and the measured earthquake ground acceleration $\ddot{X}_0(t)$, i.e.,

$$\lambda(t) = \tilde{\Lambda} \, Z(t) + \tilde{q}(t) \tag{3.29}$$

The control vector $U(t)$ can be eliminated by substituting Eq. (3.13) into Eq. (3.14),

$$Z(t) = T \, D(t-\Delta t)$$
$$+ \frac{\Delta t}{2} \, [\, \frac{\Delta t}{4} \, B \, R^{-1}B'\lambda(t) + W_1\ddot{X}_0(t) \,] \tag{3.30}$$

Instead of eliminating $Z(t)$ from Eqs. (3.12) and (3.30), the term $2 \, Q \, Z(t)$ in Eq. (3.12) is expressed as $Q[Z(t) + Z(t)]$. Then, the second term of $Z(t)$ is replaced by that given in Eq. (3.30) leading to the following result,

$$Q \left\{ Z(t) + T \, D(t-\Delta t) + \frac{\Delta t}{2} \, [\frac{\Delta t}{4} \, B \, R^{-1}B'\lambda(t) \right.$$
$$\left. + W_1\ddot{X}_0(t)] \right\} + \lambda(t) = 0 \tag{3.31}$$

Substituting Eq. (3.29) into Eq. (3.31) yields

$$\left\{ Q + \left[\frac{(\Delta t)^2}{8} Q \, B \, R^{-1}B' + I \right] \tilde{\Lambda} \right\} Z(t)$$
$$+ Q \left\{ T \, D(t-\Delta t) + \frac{\Delta t}{2} \, W_1\ddot{X}_0(t) \right\}$$
$$+ \left\{ \frac{(\Delta t)^2}{8} Q \, B \, R^{-1}B' + I \right\} \tilde{q}(t) = 0 \tag{3.32}$$

3-8

From Eq. (3.32), one obtains, for $Z(t) \neq 0$ and $\tilde{q}(t) \neq 0$, the following equations for the solution of unknown matrix $\tilde{\Lambda}$ and vector $\tilde{q}(t)$

$$Q + \left[\frac{(\Delta t)^2}{8} Q B R^{-1}B' + I \right] \tilde{\Lambda} = 0 \qquad (3.33)$$

$$Q \left[T D(t-\Delta t) + \frac{\Delta t}{2} W_1 \ddot{X}_0(t) \right]$$

$$+ \left[\frac{(\Delta t)^2}{8} Q B R^{-1}B' + I \right] \tilde{q}(t) = 0 \qquad (3.34)$$

The unknowns $\tilde{\Lambda}$ and $\tilde{q}(t)$ are obtained as follows

$$\tilde{\Lambda} = - \left[\frac{(\Delta t)^2}{8} Q B R^{-1}B' + I \right]^{-1} Q \qquad (3.35)$$

$$\tilde{q}(t) = \tilde{\Lambda}[T D(t-\Delta t) + \frac{\Delta t}{2} W_1 \ddot{X}_0(t)] \qquad (3.36)$$

Thus the control vector $U(t)$ and the response state vector $Z(t)$ under the instantaneous optimal closed-open-loop control are determined in the following:

$$U(t) = \frac{\Delta t}{2} R^{-1}B'[\tilde{\Lambda} Z(t) + \tilde{q}(t)] \qquad (3.37)$$

$$Z(t) = [I - \frac{(\Delta t)^2}{8} B R^{-1}B' \tilde{\Lambda}]^{-1} \{T D(t-\Delta t)$$

$$+ \frac{(\Delta t)^2}{8} B R^{-1}B' \tilde{q}(t) + \frac{\Delta t}{2} W_1 \ddot{X}_0(t)\} \qquad (3.38)$$

in which $\tilde{\Lambda}$ and $\tilde{q}(t)$ are given in Eqs. (3.35) and (3.36), respectively.

3.5 Determination of the Weighting Matrix Q

For the instantaneous optimal closed-loop control, the control force vector $U(t)$ depends on the weighting matrix Q as follows

$$U(t) = -(\Delta t/2) \, R^{-1} \, B' \, Q \, Z(t) \qquad (3.39)$$

in which $Z(t)$ is a 2n state vector consisting of the displacement response vector $Y(t)$ and the velocity response vector $\dot{Y}(t)$, i.e.,

$$Z'(t) = [Y'(t) : \dot{Y}'(t)] \qquad (3.40)$$

From the equation above, the control force vector $U(t)$ depends on the weighting matrices R and Q, which are prescribed (or preassigned) rather than being obtained through some criteria. As a result, an appropriate choice of the weighting matrices R and Q requires some careful considerations, in particular the elements of the (2n x 2n) Q matrix. Some pertinent features for a proper assignment of the elements of the Q matrix as well as their significance will be described in the following.

In Eq. (3.39), B is a (2n x r) matrix, the transpose of which can be expressed in a partition form

$$B' = [0 : H'(m^{-1})'] \qquad (3.41)$$

where r is the total number of controllers, 0 is a (r x n) zero matrix, m is a (n x n) diagonal mass matrix, and H is a (n x r) location matrix indicating the location of controllers [see Appendix A].

The (2n x 2n) weighting matrix Q can be partitioned into four (n x n) submatrices as follows

$$\underset{\sim}{Q} = \begin{bmatrix} \underset{\approx}{Q}_{11} & \vdots & \underset{\approx}{Q}_{12} \\ ------ & \vdots & ------ \\ \underset{\approx}{Q}_{21} & \vdots & \underset{\approx}{Q}_{22} \end{bmatrix} \qquad (3.42)$$

Substituting Eqs. (3.40) - (3.42) into Eq. (3.39), one obtains

$$\underset{\sim}{U}(t) = - (\Delta t/2) \underset{\sim}{R}^{-1} \underset{\sim}{H}' (\underset{\sim}{m}^{-1})' [\underset{\approx}{Q}_{21}\underset{\sim}{Y}(t)$$

$$+ \underset{\approx}{Q}_{22}\dot{\underset{\sim}{Y}}(t)] \qquad (3.43)$$

It follows from Eq. (3.43) that the control force vector $\underset{\sim}{U}(t)$ is independent from the (n x n) matrices $\underset{\approx}{Q}_{11}$ and $\underset{\approx}{Q}_{12}$, indicating that $\underset{\approx}{Q}_{11}$ and $\underset{\approx}{Q}_{12}$ do not affect the control system. Hence, $\underset{\approx}{Q}_{11}$ and $\underset{\approx}{Q}_{12}$ should be assigned with zero elements in order to reduce the performance index J(t).

Note that $\underset{\sim}{m}$ is a (n x n) diagonal mass matrix and hence $(\underset{\sim}{m}^{-1})'$ is also a diagonal matrix. Likewise, elements in the jth column of the location matrix $\underset{\sim}{H}$ are all zero if the controller is not installed in the jth story unit. Since $\underset{\approx}{Q}_{21}$ and $\underset{\approx}{Q}_{22}$ are premultiplied by $\underset{\sim}{H}'(\underset{\sim}{m}^{-1})'$, see Eq. (3.43), the jth row of $\underset{\approx}{Q}_{21}$ and $\underset{\approx}{Q}_{22}$ will disappear in the expression for $\underset{\sim}{U}(t)$. Consequently, elements in the jth row of $\underset{\approx}{Q}_{21}$ and $\underset{\approx}{Q}_{22}$ should be assigned with zero values if no controller is installed in the jth story unit.

In Eq. (3.43), $\underset{\approx}{Q}_{21}$ is multiplied by the measured displacement vector $\underset{\sim}{Y}(t)$, whereas $\underset{\approx}{Q}_{22}$ is multiplied by the measured velocity vector $\dot{\underset{\sim}{Y}}(t)$. Therefore, the magnitude of the elements in each column of the $\underset{\approx}{Q}_{22}$ matrix represents the relative importance (or contribution to the control force) of the corresponding velocity

sensor, and the magnitude of the elements of each column of the Q_{21} matrix denotes the relative importance of the corresponding displacement sensor. Hence, if one would like to reduce a particular displacement or velocity, then elements of the corresponding column of either Q_{21} or Q_{22} matrix should be assigned with large values.

It should be mentioned that salient features associated with the assignment of elements in the weighting matrix Q described above hold for all three instantaneous optimal control algorithms.

For the Riccati closed-loop control, the control force vector is expressed as

$$U(t) = - (1/2) \ R^{-1} \ B' \ P \ Z(t) \tag{3.43}$$

A comparison between Eqs. (3.39) and (3.43) indicates that the Riccati matrix P in the Riccati closed-loop control plays the same role as the weighting matrix Q in the instantaneous optimal closed-loop control, as far as the control force is concerned. Consequently, the following conclusions are derived from our previous discussions of the Q matrix.

(1) The (n x n) submatrices P_{11} and P_{12} have no effect whatsoever on the control force vector $U(t)$, where

$$P = \begin{bmatrix} P_{11} & \vdots & P_{12} \\ \text{------} & \vdots & \text{------} \\ P_{21} & \vdots & P_{22} \end{bmatrix} \tag{3.44}$$

(2) If the controller is not installed in the jth story unit, elements in the jth row of the $[P_{21} : P_{22}]$ matrix do not have contribution to the control force vector $U(t)$, and

(3) The magnitude of the elements in each column of the P_{21} submatrix represents the relative importance of the corresponding displacement sensor, whereas that of the P_{22} submatrix indicates the relative importance of the corresponding velocity sensor.

Unlike the instantaneous optimal closed-loop control in which elements of the weighting matrix Q are assigned, the Riccati matrix P is determined from the Riccati matrix equation. In other words, P is a function of the structural characteristics, A, the weighting matrices R and Q, and the location matrix B. In general, the Riccati matrix is a full matrix. However, from the observations made above, valuable conclusions can be derived with regard to the optimal locations for sensors and controllers in the following.

In practical applications, tall buildings usually involve many degrees of freedom, whereas the number of sensors and controllers are limited. Based on economical and design considerations, the fewer the sensors and controllers, the better. With a limited number of sensors and controllers, the question of optimal locations for a limited number of sensors and controllers is of practical importance. From the previous discussions, the optimal locations for sensors and controllers can be determined. The results of such a study for the optimal locations of sensors and controllers will be reported in the near future.

3.6 Numerical Examples

To demonstrate the applications of instantaneous optimal control algorithms developed in this chapter, several configurations of active control systems are considered in the following.

3.6.1 Example 1: Active Tendon Control System

The same eight story building in which an active tendon controller is installed in every story unit given in Chapter II

is considered. The earthquake ground acceleration is also identical to that considered in Section II. With the simulated earthquake ground acceleration shown in Fig. 2.3 as input, the top floor relative displacement and the base shear force of the building without the active control system are presented in Figs. 3.1(a) and 3.2(a).

For the Riccati closed-loop control, the weighting matrices Q and R are chosen to be diagonal with elements Q_{ii} = 10^5 (i=1,2,...,8), Q_{ii} = 0 (i=9,10,...,16), and R_{ii} = 10^{-4} (i=1,2,...8). The building response quantities and the required active control force from the first controller are shown in Figs. 3.1(b), 3.2(b), and 3.3(a).

With the instantaneous optimal control algorithms, the weighting matrix $\underset{\sim}{R}$ is identical to the one given above. However, the (16x16) weighting matrix $\underset{\sim}{Q}$ is partitioned as follows

$$\underset{\sim}{Q} = \alpha \left[\begin{array}{c:c} \underset{\sim}{0} & \underset{\sim}{0} \\ \hdashline \underset{\approx}{Q}_{21} & \underset{\approx}{Q}_{22} \end{array} \right] \qquad (3.45)$$

in which $\underset{\approx}{Q}_{21}$ and $\underset{\approx}{Q}_{22}$ are (8x8) matrices and α is a constant. As described previously, the submatrices $\underset{\approx}{Q}_{11}$ and $\underset{\approx}{Q}_{12}$ do not contribute to the active control forces and hence they are chosen to be zero.

For simplicity, $\underset{\approx}{Q}_{21}$ and $\underset{\approx}{Q}_{22}$ are chosen to be equal, i.e., $\underset{\approx}{Q}_{21}$ = $\underset{\approx}{Q}_{22}$ = $\underset{\sim}{Q}^*$. The elements of $\underset{\sim}{Q}^*$, denoted by $\underset{\sim}{Q}^*(i,j)$, are chosen in the following manner.

$$Q^*(i,j) = \begin{array}{ll} j & \text{for } i > j \\ i & \text{for } i \le j \end{array} \qquad (3.46)$$

Note that guidelines for assigning values to elements $\underset{\sim}{Q}^{*}(i,j)$ have not been established in the literature. There is no particular reason for the choices of $\underset{\sim}{Q}^{*}(i,j)$ given by Eq. (3.46), except to mention that it is based on experience and intuition. For a 69% reduction of the building response, a value of 4200 is used for α.

The building response quantities are displayed in (c), (d), and (e) of Figs. 3.1-3.2, respectively, for the instantaneous optimal closed-loop control, intantaneous optimal open-loop control, and instantaneous optimal closed-open-loop control. The corresponding required active control forces from the first controller are depicted in Fig. 3.3(b), (c) and (d). It is observed that the building response quantities as well as the required active control forces are all identical under three instantaneous optimal control algorithms. This has been expected because each control algorithm is derived by minimizing the same objective function (performance index). The maximum response quantities and the maximum control force from the first controller are summarized in Table 3.1. It is observed from Figs. 3.1 to 3.3 and Table 3.1 that the control efficiency is almost identical for both the Riccati closed-loop control and the instantaneous optimal control under this particular situation.

Suppose only 4 active tendon controllers are installed in the lowest four story units. For the Riccati closed-loop control, the (4x4) weighting matrix $\underset{\sim}{R}$ is considered a diagonal matrix with $R_{11} = R_{22} = R_{33} = R_{44} = 10^{-4}$. The (16x16) weighting matrix $\underset{\sim}{Q}$ is again a diagonal matrix with $Q_{ii} = 1.3 \times 10^{5}$ for $i = 1,2,3,4$ and $\underset{\sim}{Q}_{jj} = 0$ for $j = 5,6,7,8$. The response quantities and the required active control force from the first controller are depicted in Figs. 3.4(b), 3.5(b), and 3.6(a).

For the instantaneous optimal control algorithms, the same $\underset{\sim}{R}$ matrix given above is used. However, the $\underset{\sim}{Q}$ matrix is subdivided into (8x8) submatrices as given by Eq. (3.45) with $\underset{\sim}{Q}_{21} = \underset{\sim}{Q}_{22} = \underset{\sim}{Q}^*$. The elements of $\underset{\sim}{Q}^*$, denoted by $Q^*(i,j)$, is chosen as follows

$$Q^*(i,j) = \begin{cases} j & \text{for} \quad i \leq 4 \\ 0 & \text{for} \quad i > 4 \end{cases} \qquad (3.47)$$

for $i = 1,2,\ldots,8$ and $j = 1,2,\ldots,8$. For a 68% reduction of the response quantities, a value of 5,000 is chosen for α, see Eq. (3.45). The response quantities and the required active control force from the first controller using various instantaneous optimal control algorithms are displayed in Figs. 3.4-3.6. The maximum responses and the required active control force are summarized in Table 3.2. Again the efficiency of the Riccati closed-loop control is almost identical to that of various instantaneous optimal control algorithms.

3.6.2 Example 2: Active Mass Damper Control System

An active mass damper control system installed on the top of the same 8-story building is considered, see Fig. 3.7. The properties of the active mass damper are: m_d = mass of the damper = 29.63 tons, c_d = damping of the damper = 25. tons/sec, k_d = stiffness of the damper = 957.2 KN/m. Note that the mass m_d is 2% of the generalized mass associated with the first vibrational mode, the frequency of the damper is 98% of the first natural frequency of the building, and the damping ratio of the damper is approximately 7.3%. In the present example, the weighting matrix $\underset{\sim}{R}$ consists of only one element, i.e., $\underset{\sim}{R} = \underset{\sim}{R}^*$, whereas the dimension of the $\underset{\sim}{Q}$ matrix is (18x18).

Without the active control force, the mass damper is passive. For the passive mass damper and with the simulated ground

acceleration shown in Fig. 2.3 as an input, the top floor relative displacement and the base shear force are shown in Figs. 3.8(a) and 3.9(a), respectively.

With the application of the Riccati closed-loop control, the weighting matrix $\underset{\sim}{Q}$ is considered to be a diagonal matrix with Q_{ii} = 1.3 x 10^5 (for i=1,2,...,8), and Q_{jj} = 0 (for j=9,10,...,18). The element of $\underset{\sim}{R}$ matrix is $R^* = 10^{-3}$. The top floor relative displacement, the base shear force and the required active control force are displayed in Figs. 3.8(b), 3.9(b) and 3.10(a), respectively.

In applying various instantaneous optimal control laws, the same R matrix is used. However, the active control force is influenced only by the last two rows of the weighting matrix $\underset{\sim}{Q}$. Thus, only the elements in the last two rows will be assigned with some values, i.e.,

$$\underset{\approx}{Q} = \alpha \begin{bmatrix} \underset{\sim}{0} & : & \underset{\sim}{0} \\ \hline \underset{\approx}{Q}_{21} & : & \underset{\approx}{Q}_{22} \end{bmatrix} \qquad (3.48)$$

in which $\underset{\approx}{Q}_{21}$ and $\underset{\approx}{Q}_{22}$ are (2x9) matrices. For illustrative purpose these two matrices are given in the following:

$$\underset{\approx}{Q}_{21} = \begin{bmatrix} -33.5 & -67 & -100.5 & -134 & -167.5 & -201 & -234.5 & -268 & 375.6 \\ -33.5 & -67 & -100.5 & -134 & -167.5 & -201 & -234.5 & -268 & 32.2 \end{bmatrix}$$

$$\underset{\approx}{Q}_{22} = \begin{bmatrix} 67.5 & 135 & 202.5 & 270 & 338.5 & 405 & 472.5 & 540 & 32.2 \\ 5.8 & 11.6 & 17.4 & 23.2 & 29 & 34.7 & 40.5 & 46.3 & 5.7 \end{bmatrix}$$

A value of 67.0 is chosen for α such that the top floor relative displacement is reduced by approximately 60%.

By using the weighting matrices described above and the application of various instantaneous optimal control algorithms, the top floor relative displacement, the base shear force and the required active control force are depicted in Figs. 3.8, 3.9, and 3.10. The maximum values in the time histories of the response quantities and the active control force within 30 seconds are summarized in Table 3.3. As expected, the three instantaneous optimal control algorithms produce identical results. Figs. 3.8-3.10 and Table 3.3 indicate that the instantaneous optimal control algorithms are slightly more efficient than the Riccati closed-loop control.

It is well known that the weighting matrices should be chosen such that R is positive definite and Q is positive semi-definite. However, the appropriate assignment of elements of Q and R matrices has not been discussed in the literature, in particular how to choose elements of Q and R matrices to achieve the maximum control efficiency. This is a subject of future research.

TABLE 3.1: Maximum Structural Responses and Control Force
            For 8-Story Building With 8 Controllers

CONTROL LAW	TOP FLOOR DISPLACEMENT (CM)	BASE SHEAR FORCE (KN)	CONTROL FORCE FROM 1ST CONTROLLER (KN)
Uncontrol	4.10	2,506	----------
Riccati closed-loop control	1.31	907	364
Instantaneous optimal control	1.29	894	361

TABLE 3.2:   Maximum Structural Responses and Control Force
For 8-Story Building With 4 Controllers

CONTROL LAW	TOP FLOOR DISPLACEMENT (CM)	BASE SHEAR FORCE (KN)	CONTROL FORCE FROM 1ST CONTROLLER (KN)
Uncontrol	4.10	2,506	----------
Riccati closed-loop control	1.36	853	437
Instantaneous optimal control	1.34	847	421

TABLE 3.3: Maximum Structural Responses and Control Force
For 8-Story Building With Active Mass-Damper

CONTROL LAW	TOP FLOOR DISPLACEMENT (CM)	BASE SHEAR FORCE (KN)	ACTIVE CONTROL FORCE (KN)
Uncontrol	4.10	2,506	----------
Riccati closed-loop control	1.61	1,075	250
Instantaneous optimal control	1.54	1,045	232
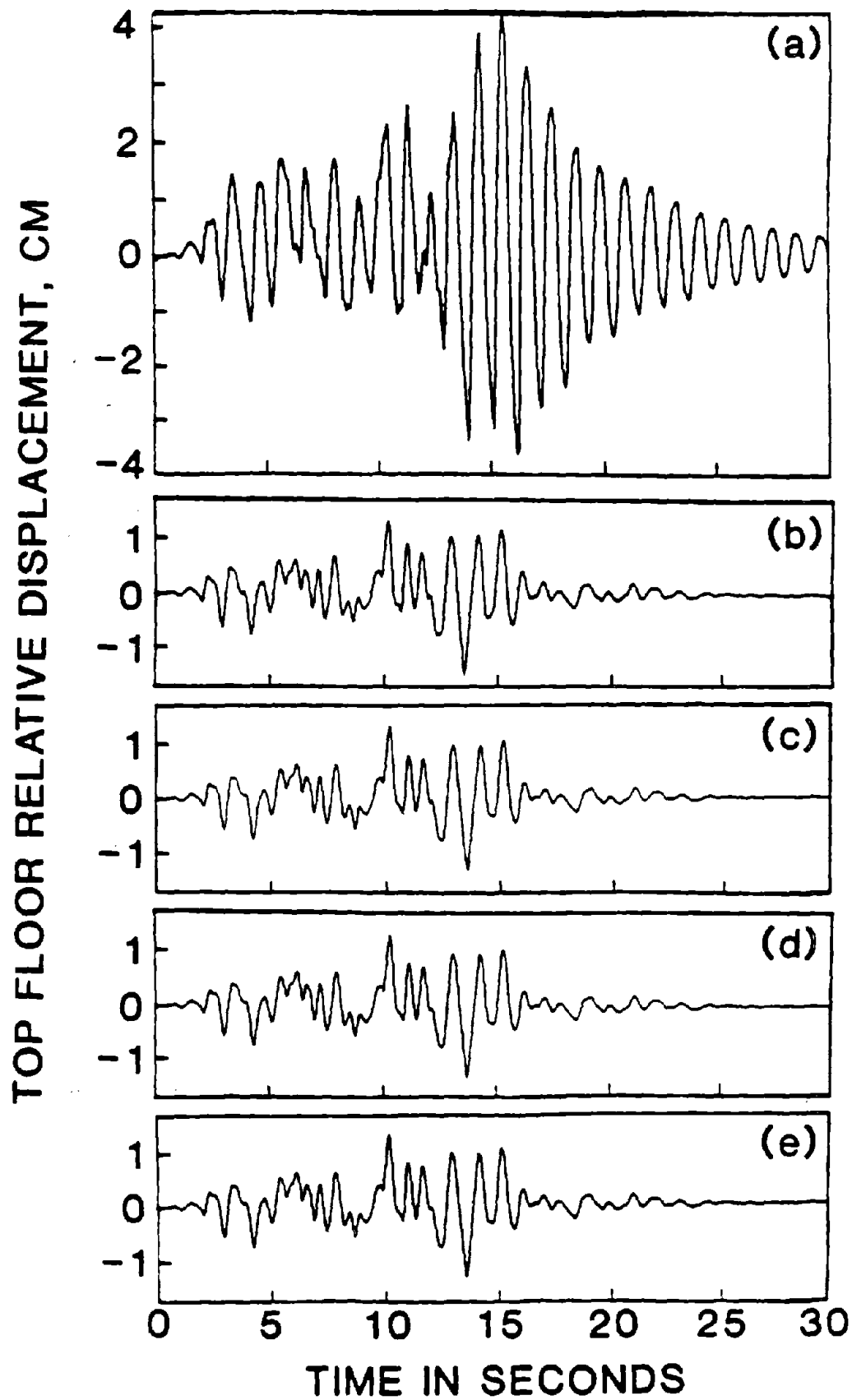
FIGURE 3-1   Top Floor Relative Displacement for a 8-Story Building With 8
Tendon Controllers; (a) No Control, (b) Riccati Closed-Loop
Control, (c) Instantaneous Optimal Closed-Loop Control, (d)
Instantaneous Optimal Closed-Open Loop Control.
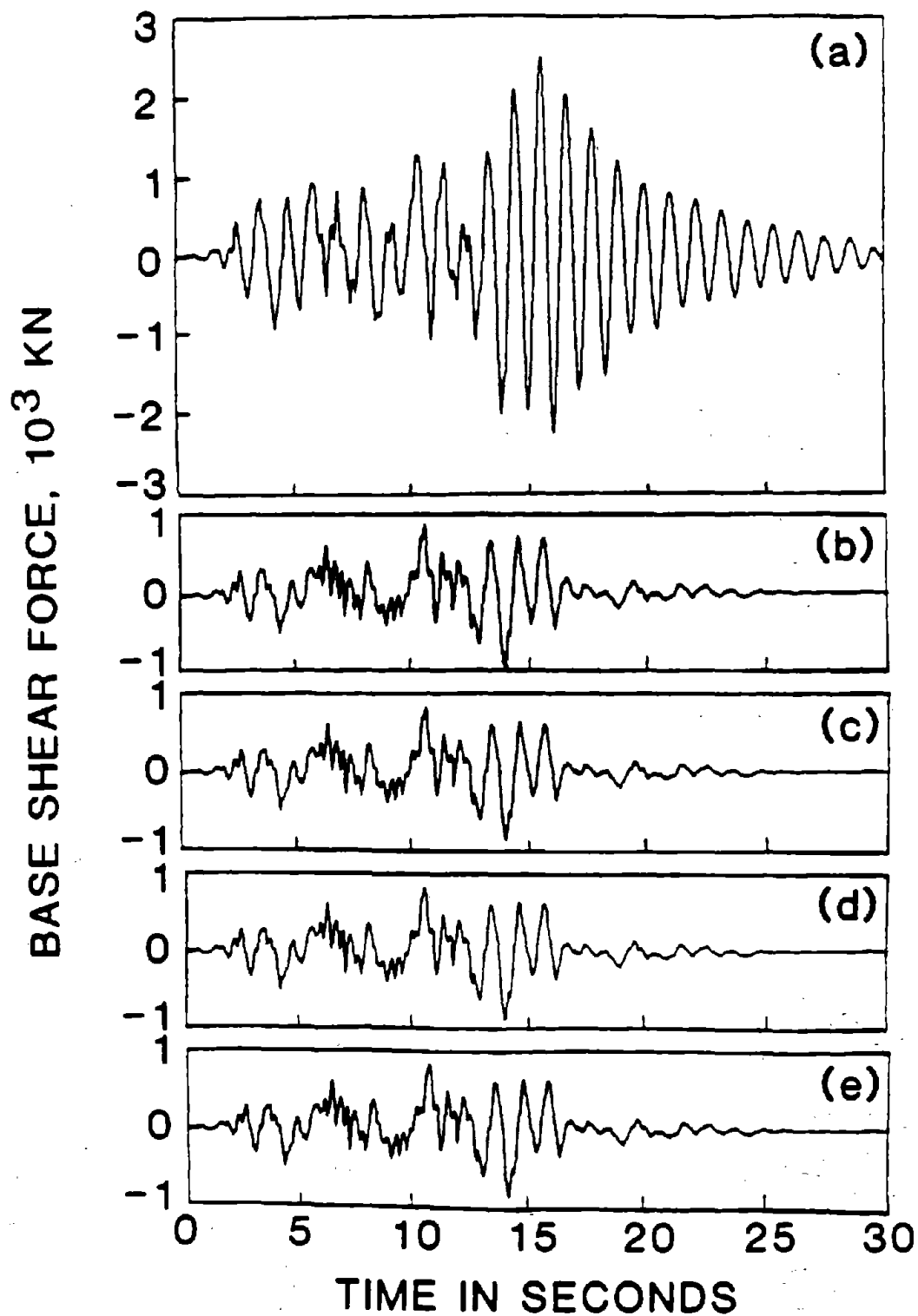
FIGURE 3-2   Base Shear Force For a 8-Story Building With 8 Tendon
Controllers; (a) No Control, (b) Riccati Closed-Loop Control, (c)
Instantaneous Optimal Closed-Loop Control, (d) Instantaneous
Optimal Closed-Open Loop Control.

3-23
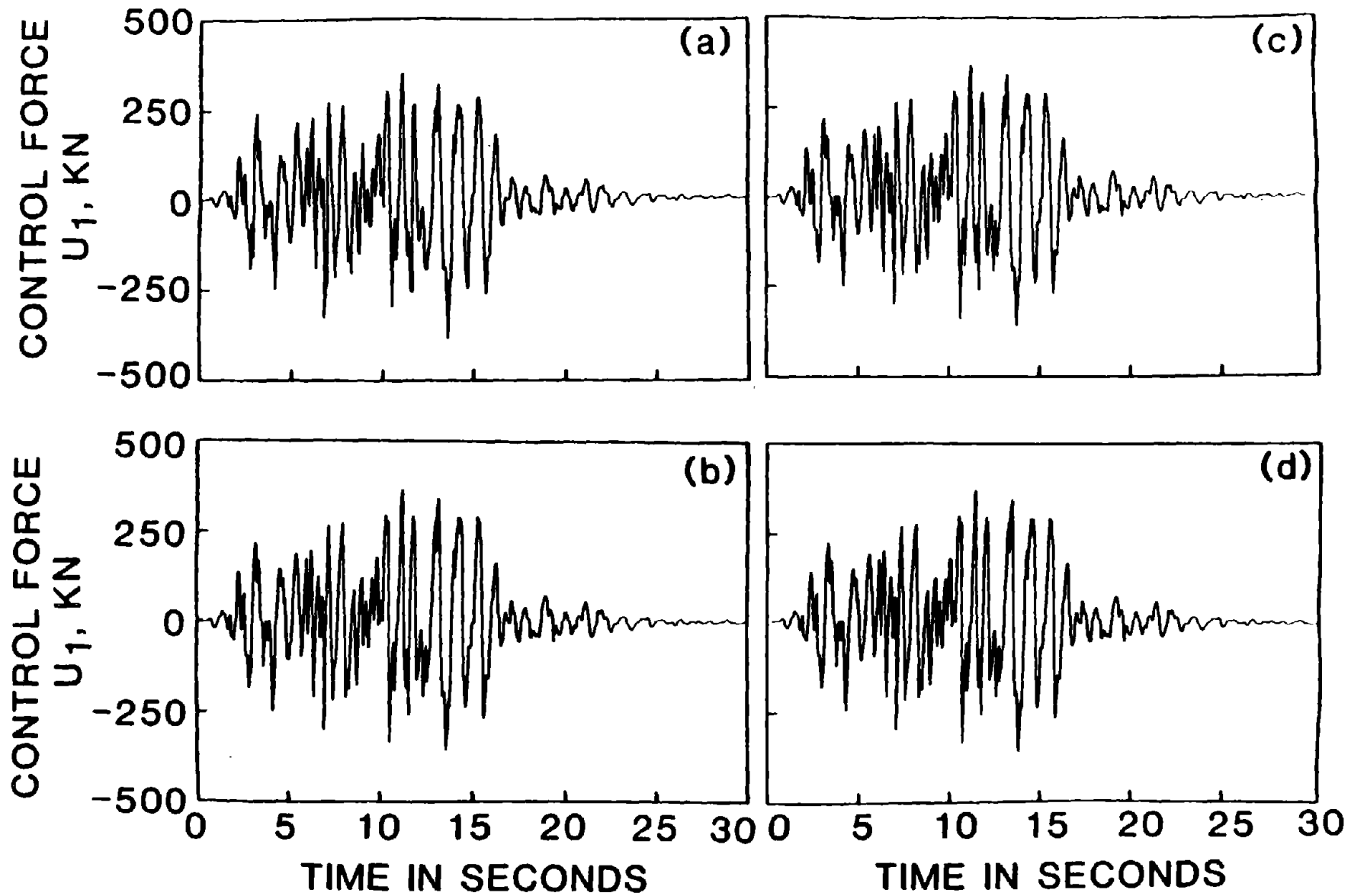
FIGURE 3-3   Active Control Force From the First Controller For a 8-Story
Building With 8 Tendon Controllers: (a) Riccati Closed-Loop
Control, (b) Instantaneous Optimal Closed-Loop Control, (c)
Instantaneous Optimal Open-Loop Control, (d) Instantaneous
Optimal Closed-Loop Control.
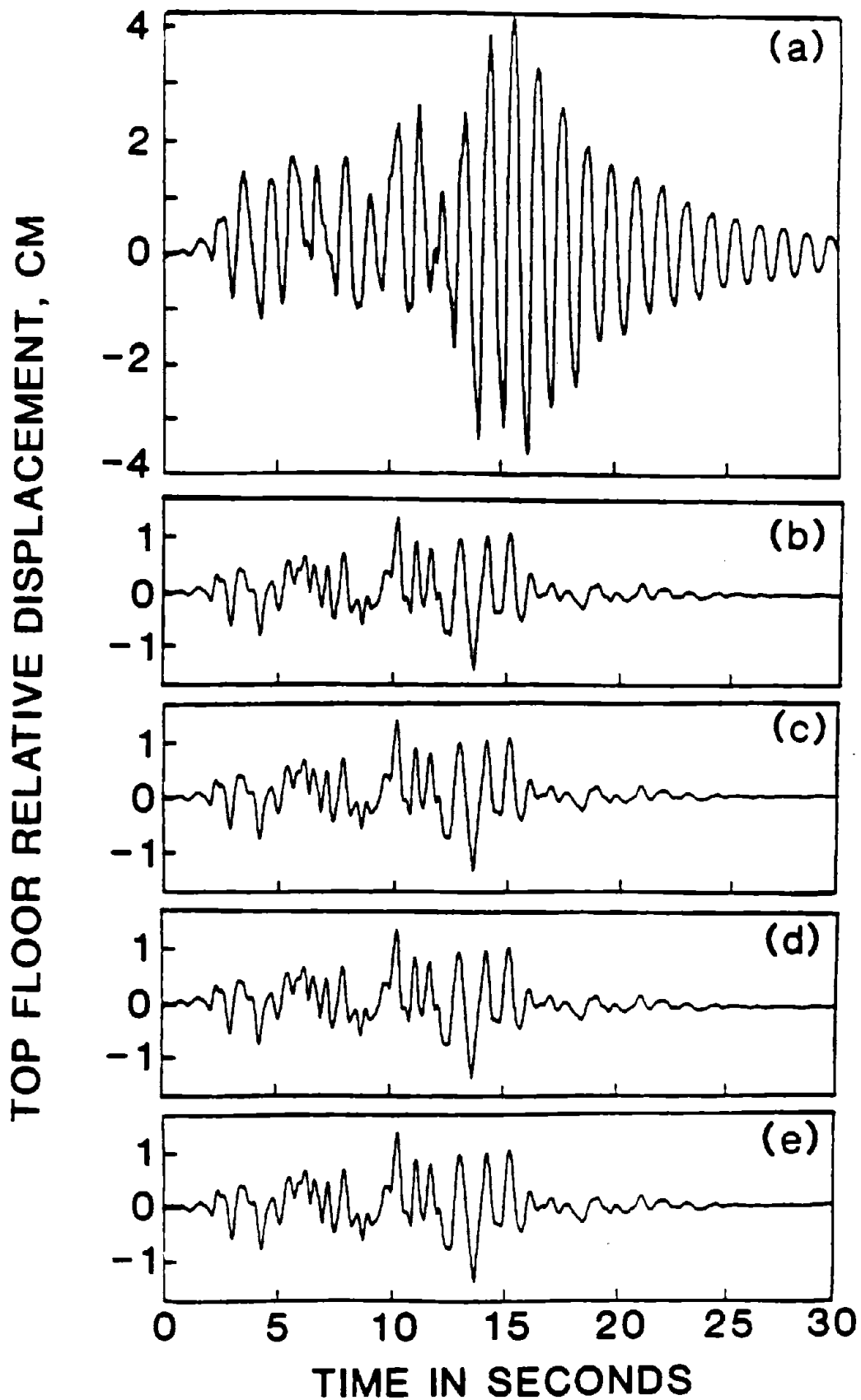
FIGURE 3-4   Top Floor Relative Displacement for a 8-Story Building with 4
Tendon Controllers; (a) No Control, (b) Riccati Closed-Loop
Control, (c) Instantaneous Optimal Closed-Loop Control, (d)
Instantaneous Optimal Open-Loop Control, (e) Instantaneous
Optimal Closed-Open Loop Control.

3-25
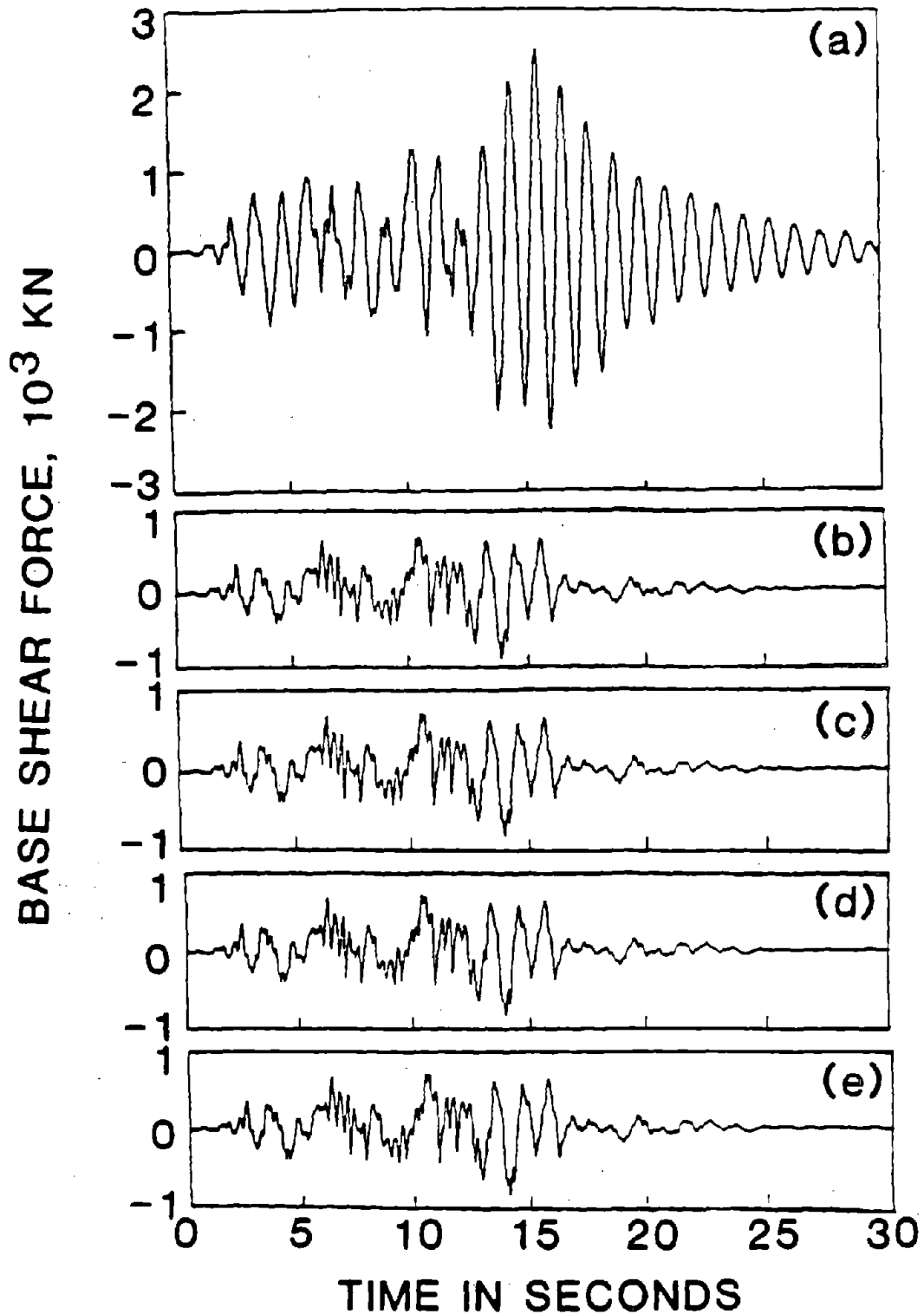
FIGURE 3-5   Base Shear Force For a 8-Story Building With 4 Tendon
Controllers: (a) No Control, (b) Riccati Closed-Loop Control, (c)
Instantaneous Optimal Closed-Loop Control, (d) Instantaneous
Optimal Open-Loop Control, (e) Instantaneous Optimal
Closed-Open Loop Control.
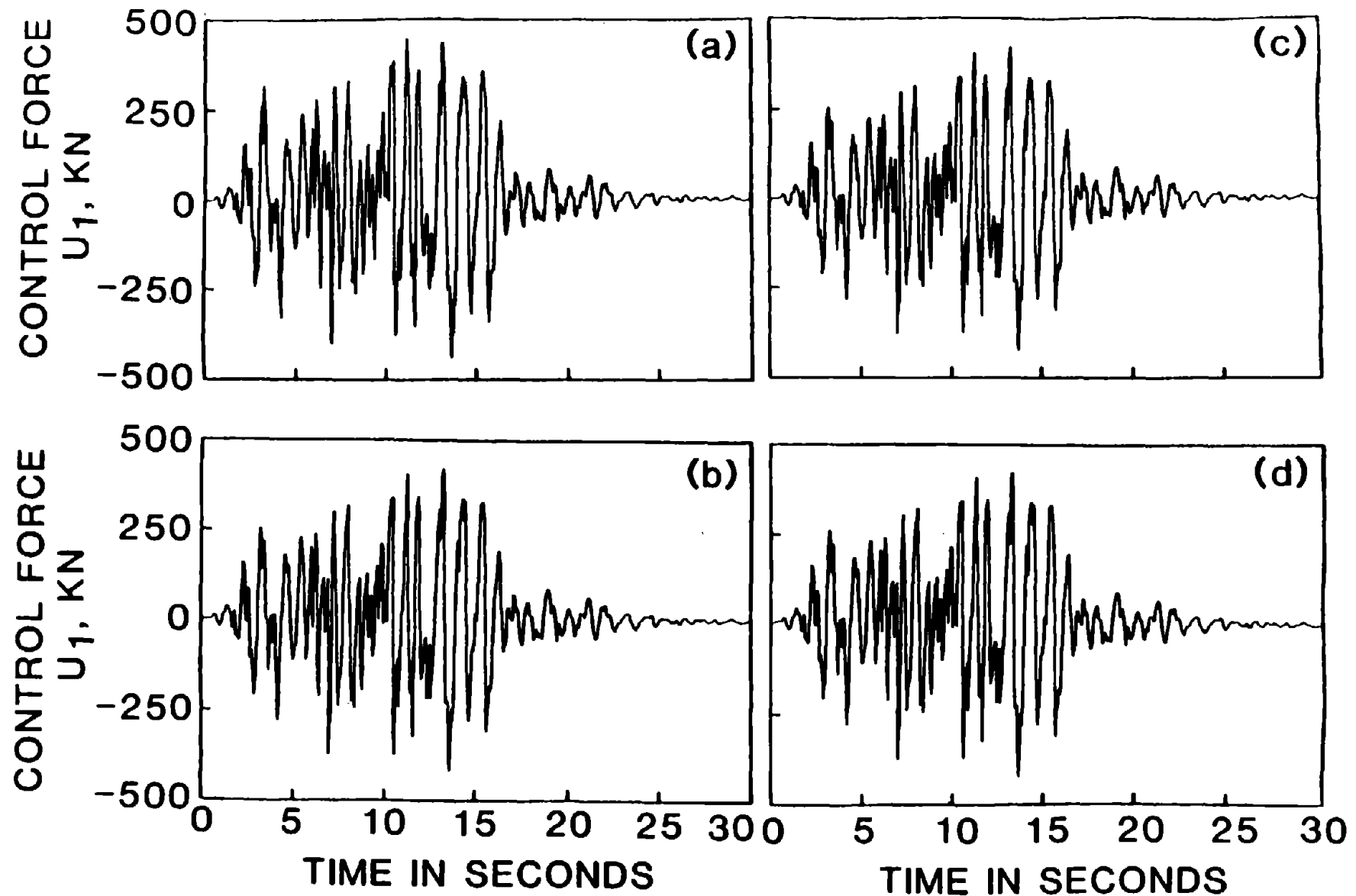
FIGURE 3-6 Active Control Force From the First Controller For a 8-Story Building With 4 Tendon Controllers: (a) Riccati Closed-Loop Control, (b) Instantaneous Optimal Closed-Loop Control, (c) Instantaneous Optimal Open-Loop Control, (d) Instantaneous Optimal Closed-Open Loop Control.
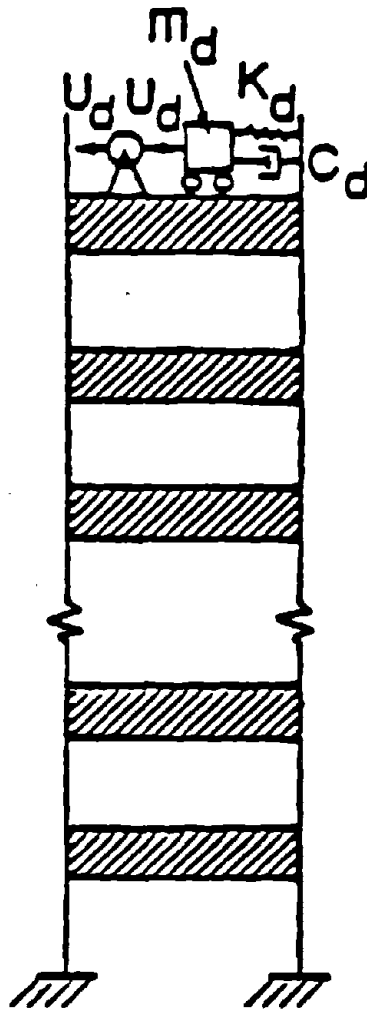
FIGURE 3-7 Structural Model of a Multi-Story Building With an Active Mass
Damper Control System.
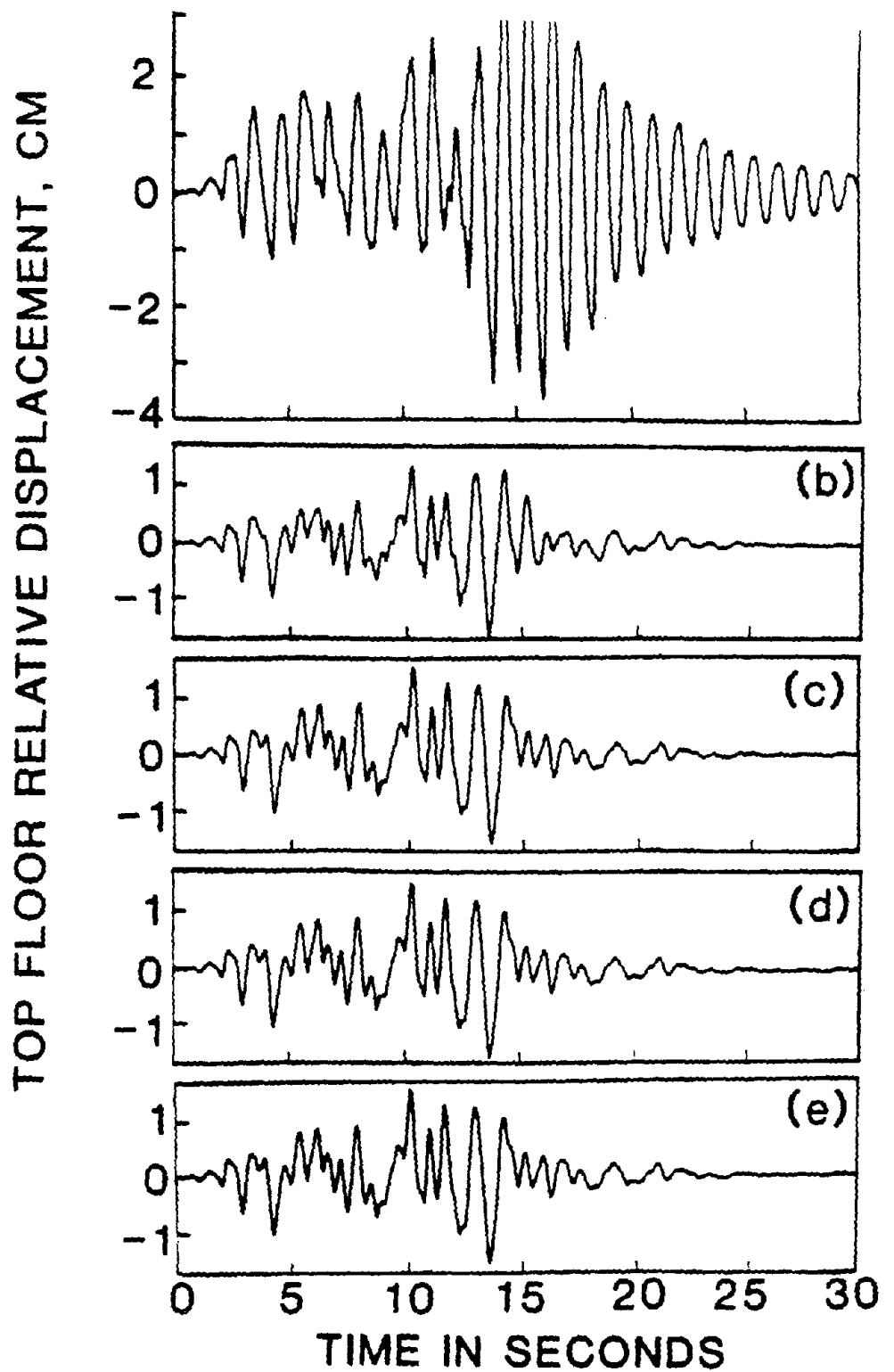
FIGURE 3-8   Top Floor Relative Displacement for an 8-Story Building with Active Mass Damper Control System: (a) Passive Mass Damper, (b) Riccati Closed-Loop Control, (c) Instantaneous Optimal Closed-Loop Control, (d) Instantaneous Optimal Open-Loop Control, (e) Instantaneous Optimal Closed-Open-Loop Control.

3-29
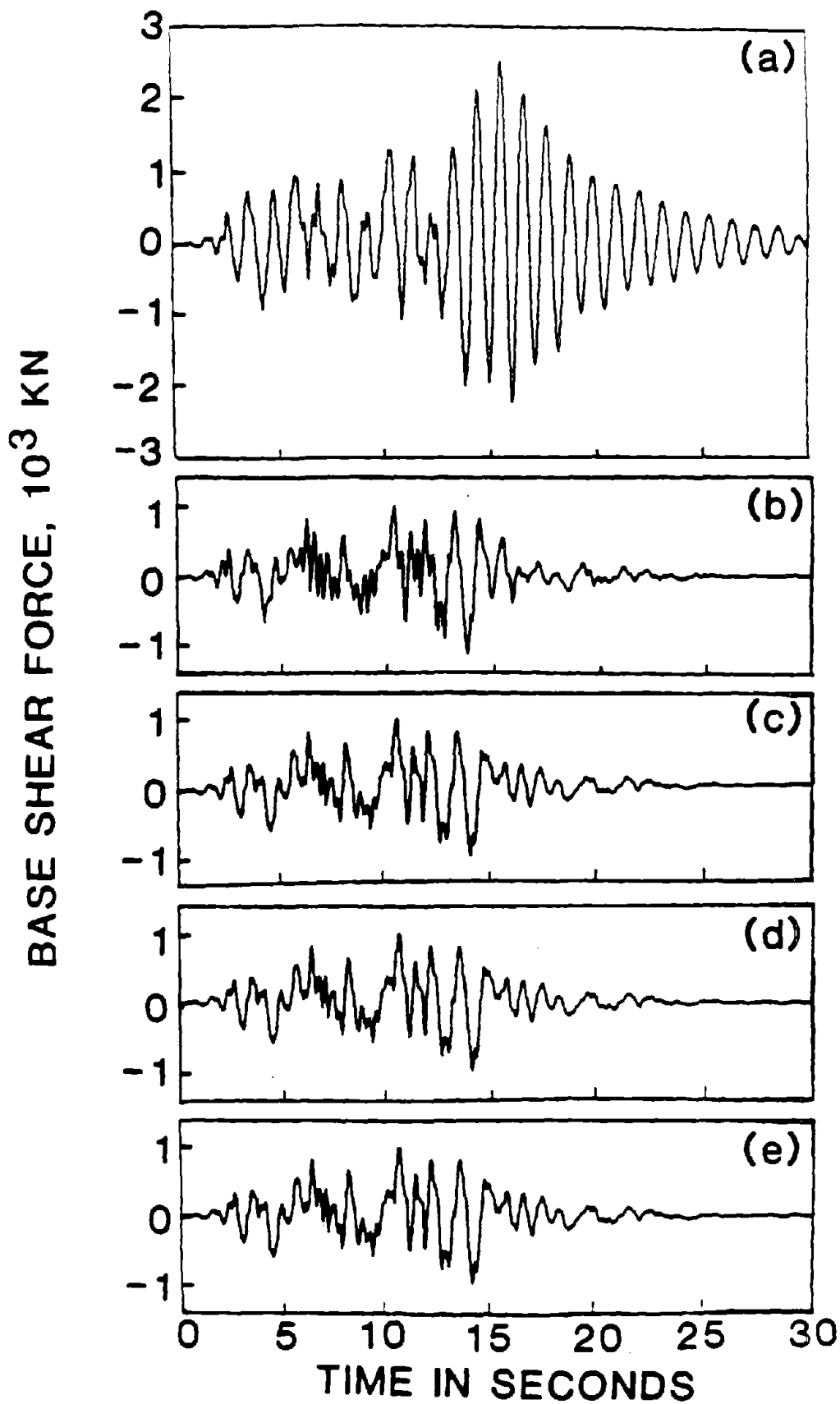
FIGURE 3-9   Base Shear Force for an 8-Story Building With an Active Mass Damper Control System: (a) Passive Mass Damper, (b) Riccati Closed-Loop Control, (c) Instantaneous Optimal Closed-Loop Control, (d) Instantaneous Optimal Open-Loop Control, (e) Instantaneous Optimal Closed-Open-Loop Control.
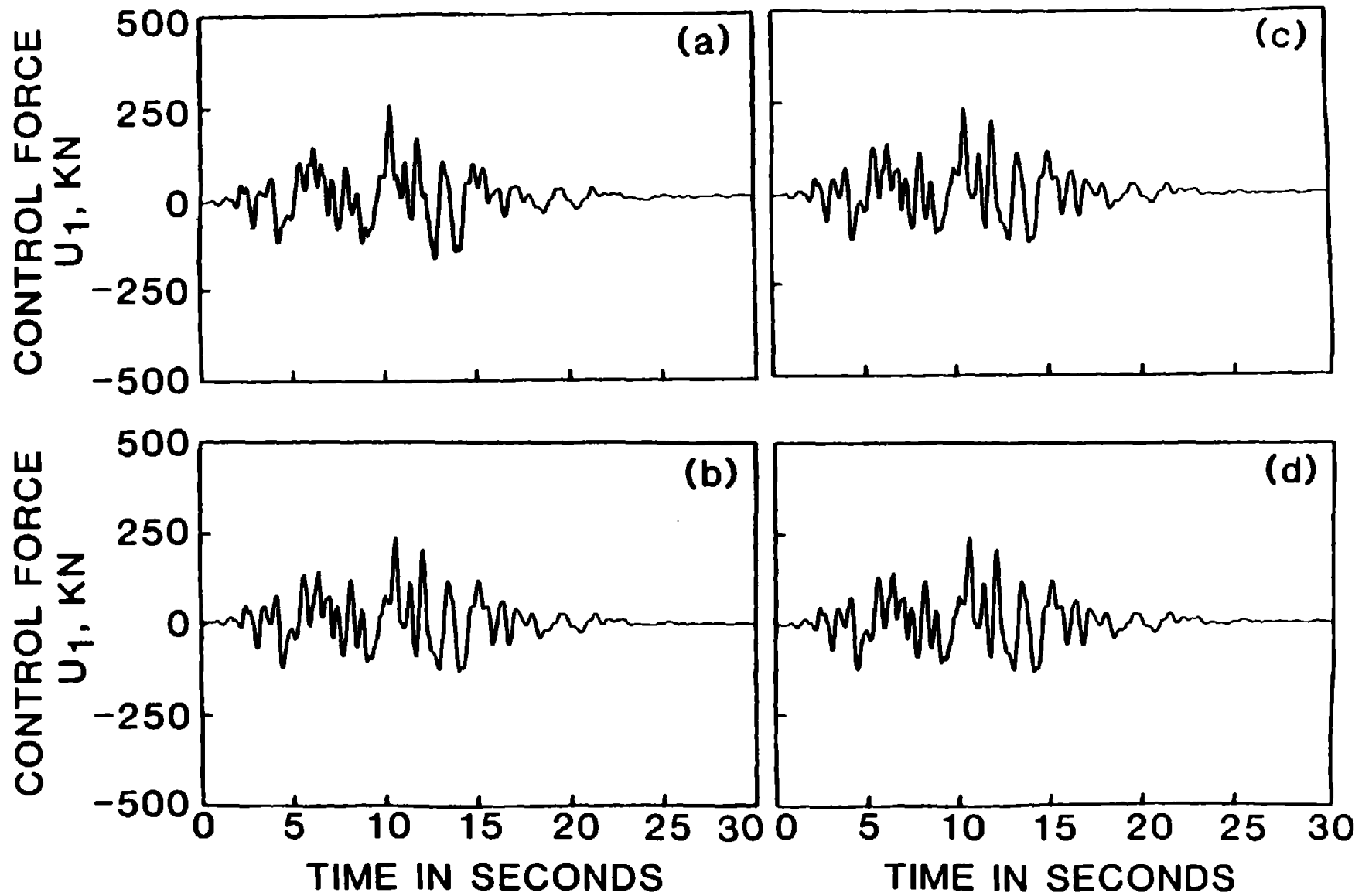
FIGURE 3-10   Active Control Force For Mass-Damper: (a) Riccati Closed-Loop
Control, (b) Instantaneous Optimal Closed-Loop Control, (c)
Instantaneous Optimal Open-Loop Control, (d) Instantaneous
Optimal Closed-Open Loop Control.

SECTION 4
CONCLUSIONS

Under earthquake excitations it is demonstrated that the Riccati closed-loop control does not satisfy the optimal condition. The optimal closed-open-loop control and optimal open-loop control algorithms are shown to be superior to the Riccati closed-loop control. However, the former two control algorithms are not feasible for applications to earthquake engineering problems because the complete history of the earthquake ground motion is not known a priori. Thus, only the closed-loop control algorithms are applicable to earthquake-excited structures, such as the Riccati matrix approach, pole assignment [e.g. 2, 17, 20], sub-optimal control [e.g., 39-41, 56], etc. The pole assignment method is rather cumbersome for complex building structures with many degrees of freedom [e.g., 17]. Furthermore, it is not clear where the poles (eigenvalues) of the structure should be assigned, because the future earthquake excitation is not known a priori.

Utilizing the information of the earthquake ground motions measured by installing sensors on the basement, three new optimal control algorithms have been proposed in this report. The new objective function to be minimized is a time dependent performance index expressed in terms of quadratic functions. Since the performance index is minimized at every time instant, the algorithms developed herein are referred to as the instantaneous optimal control algorithms. These include the instantaneous optimal closed-loop control, instantaneous optimal open-loop control, and instantaneous optimal closed-open-loop control. The control efficiencies for these three instantaneous optimal control laws are identical under ideal operational environments. The efficiency of the Riccati closed-loop control algorithm is compared with that of the instantaneous optimal control algorithms using two numerical examples; one with the

application of the active tendon control system, and the other with the active mass damper.

Numerical results indicate that the proposed instantaneous optimal control laws are slightly more efficient than the Riccati closed-loop control law. However, the newly proposed instantaneous optimal control laws are easier to be implemented. For instance, the gain matrix for the instantaneous optimal closed-loop control does not require any computational effort, and it is independent of structural characteristics and parameters. Thus, the instantaneous optimal closed-loop control algorithm is independent of the uncertainty in structural identification. On the other hand, the computation of the Riccati matrix can be very cumbersome and time consuming for a tall building with a large number of degrees of freedom. Likewise, since the Riccati matrix is a function of the structural parameters, the control system is sensitive to the structural identification that usually involves considerable uncertainty.

The three instantaneous optimal control laws presented in this report were developed and proposed by the authors in 1985 and then transmitted to their co-workers at the State University of New York at Buffalo for experimental verification. Using a scaled structural model and simulating earthquake ground acceleration on the shaking table, experimental verifications for the feasibility of these three instantaneous optimal control laws have been completed recently. The results were published in Ref. 47. Meanwhile, these new control laws have been presented at a conferences [Ref. 59] and other researchers have attempted to apply them in other applications.

SECTION 5

REFERENCES

1. Abdel-Rohman, M., and Leipholz, H. H., "Active Control of Flexible Structures," Journal of the Structural Division, ASCE, Vol. 104, 1978, pp. 1251-1266.

2. Abdel-Rohman, M., and Leipholz, H. H., "Structural Control by Pole Assignment Method," Journal of the Engineering Mechanics Division, ASCE, Vol. 104, EM5, Oct. 1978, pp. 1007-1923.

3. Abdel-Rohman, M., and Leipholz, H. H., "A General Approach to Active Structural Control," Journal of the Engineering Mechanics Division, ASCE, Vol. 105, EM6, Dec. 1979, pp. 1007-1923.

4. Abdel-Rohman, M., and Leipholz, H. H., and Quintana, V. H., "Design of Reduced-Order Observers for Structural Control Systems," Structural Control, edited by H. H. Leipholz, North-Holland Publishing Company, 1980, pp. 57-78.

5. Abdel-Rohman, M., Quintana, V. H., and Leipholz, H. H., "Optimal Control of Civil Engineering Structures," Journal of Engineering Mechanics Division, ASCE, Vol. 106, EM1, Feb. 1980, pp. 57-73.

6. Abdel-Rohman, M., and Leipholz, H. H., "Automatic Active Control of Structures," Journal of the Structural Division, ASCE, Vol. 106, ST3, March 1980, pp. 663-677.

7. Abdel-Rohman, M., and Leipholz, H. H., "Structural Control Considering Time Delay Effect," accepted for publication in Transactions of the Canadian Society of Mechanical Engineers, Oct. 1984.

8. Abdel-Rohman, M., "The Feasiblity of Active Control of Tall Buildings," Second International Symposium on Structural Control, Univ. of Waterloo, Ontario, Canada, July 15-17, 1985.

9. Basharkhah, M. A., and Yao, J. T. P., "Reliability Aspects of Structural Control," Civil Engineering Systems, Vol. 1, June 1984, pp. 224-229.

10. Carotti, A., De Miranda, M., and Turci, E., "An Active Protection System for Wind Induced Vibrations of Pipeline Suspension Bridges," Second International Symposium on Structural Control, Univ. of Waterloo, Ontario, Canada, July 15-17, 1985.

11. Chang, M. I. J., and Soong, T. T., "Optimal Control Configuration for Control of Complex Structures," Structural

Control, edited by H. H. Leipholz, North-Holland Publishing Company, 1980.

12. Chang, J. C. H., and Soong, T. T., "The Use of Aerodynamic Appendages for Tall Building Control," Structural Control, edited by H. H. Leipholz, North-Holland Publishing Company, 1980, pp. 199-210.

13. Chang, J. C. H., and Soong, T. T., "Structural Control Using Active Tuned Mass Damper," Journal of the Engineering Mechanics Divison, ASCE, Vol. 106, 1980, pp. 1091-1098.

14. Dehghanyar, T. J., Masri, S. F., Miller, R. K., and Cuaghey, T. K., "On-Line Parameter Control of Nonlinear Flexible Structures," Second International Symposium on Structural Control, Univ. of Waterloo, Ontario, Canada, July 15-17, 1985.

15. Ghaemmaghami, P., and Yang, J. N., "Control of Long-Span Bridge to Wind Excitation," Proc. of the 4th International Conference on Structural Reliability and Safety, Kobe, Japan, May 1985, pp. III-213-222.

16. Goldberg, J. E., Tang, J. P., and Yao, J. T. P., "Reliability of Structures with Control Systems," Proc. Int. Sympo. Syst. Engng., Purdue University, October 23-27, 1972, Vol. 2, pp. 153-155.

17. Juang, J. N., Sae-Ung, S., and Yang, J. N., "Active Control of Large Building Structures," Structural Control, edited by H. H. Leipholz, North-Holland Publishing Company, 1980, pp. 663-676.

18. Klein, R. E., and Salhi, H., "The Time-Optimal Control of Wind Induced Structural Vibrations Using Active Appendages," Structural Control, edited by H. H. Leibholz, North-Holland Publishing Company, 1980, pp. 415-430.

19. Klein, R. E., Cusano, C., and Slukel, J. V., "Investigation of Method to Stabilize Wind Induced Oscillations in Large Structures," presented at the 1972 ASME Winter Meeting, paper No. 72-W+/AUT-11, New York, Nov. 1972.

20. Leipholz, H. H. (ed.), Structural Control, North-Holland Publishing Company, 1980.

21. Lund, R. A., "Active Damping of Large Structures in Winds," Structural Control, edited by H. H. Leipholz, North-Holland Publishing Company, 1980, pp. 459-470.

22. Lund, R. A., "Motion Control of Large Structures by Use of Active Mass Damper," ASCE 1979 Convention in Boston.

23. Martin, C. R., and Soong, T. T., "Model Control of Multistory Structures," Journal of Engineering Mechanics Division, ASCE, Vol. 102, No. EM4, Aug. 1976, pp. 613-632.

24. Masri, S. F., Bekey, G. A., Safford, F. G., and Dehghanyar, T. J., "Anti-Earthquake Application of Pulse Generators," Dynamic Response of Structures, ed. G. C. Hart, ASCE, 1981, pp. 87-101.

25. Masri, S. F., Bekey, G. A., and Caughey, T. K., "Optimum Pulse Control of Flexible Structures, Journal of Applied Mechanics, ASME, Vol. 48, 1981, pp. 619-626.

26. Masri, S. F., Bekey, G. A., and Udwadia, F. E., "On-Line Pulse Control of Tall Buildings," Structural Control, edited by H. H. Leibholz, North-Holland Publishing Company, 1980, pp. 471-492.

27. Meirovitch, L., and Gosh, D., "Control of Flutter in Bridges," Second International Symposium on Structural Control, Univ. of Waterloo, Ontario, Canada, July 15-17, 1985.

28. Meirovitch, L., and Oz, H., "Active Control of Structures by Modal Synthesis," Structural Control, edited by H. H. Leipholz, North-Holland Publishing Company, 1980, pp. 505-521.

29. Murata, M., and Ito, N., "Suppression of Wind-Induced Vibration of a Suspension Bridge by Means of a Gyroscope," Proceedings 3rd International Conference on Wind Effects on Buildings and Structures, Tokyo, Japan, 1971, pp. 1057-1066.

30. Nordell, W. J., "Active Systems for Elastic-Resistant Structures," Technical Report R-611, Naval Civil Engineering Laboratory, Port Hueneme, California, Feb. 1969.

31. Peterson, N. R., "Design of Large Scale Tuned Mass Dampers," Structural Control, edited by H. H. Leipholz, North-Holland Publishing Company, pp. 581-596.

32. Peterson, N. R., "Design Consideration of Large-Scaled Tuned Mass Damper for Structural Motion Control," ASCE 1979 Convention in Boston.

33. Peyrot, A. H., "Active Earthquake Isolation Systems," presented at the April 22-26, 1974 ASCE National Structural Engineering Meeting held at Cincinnati, Ohio, (preprint 2215).

34. Reinhorn, A. M., and Manolis, G. D., "An On-Line Control Algorithm for Inelastic Structures," Second International Symposium on Structural Control, Univ. of Waterloo, Ontario, Canada, July 15-17, 1985.

35. Roorda, J., "Experiments in Feedback Control of Structures," Structural Control, ed. by H. H. Leipholz, North-Holland Publishing Company, 1980, pp. 629-662.

36. Roorda, J., "Tendon Control in Tall Structures," Journal of the Structural Division, ASCE, Vol. 101, No. ST3, March 1975, pp. 505-521.

37. Roorda, J., "Active Damping in Structures," Granfield Report Aero., No. 8, Granfield Institute of Technology, Granfield, U.K., 1971.

38. Sae-Ung, S., and Yao, J. T. P., "Active Control of Building Structures," Journal of Engineering Mechanics Division, ASCE, Vol. 104, No. EM2, April 1978, pp. 335-350.

39. Samali, B., Yang, J. N., and Yeh, C. T., "Control of Lateral-Torsional Motion of Wind-Excited Buildings," Journal of Engineering Mechanics Division, ASCE, Vol. 111, No. 6, June 1985, pp. 777-796.

40. Samali, B., Yang, J. N., and Yeh, C. T., "Active Tendon Control System for Wind-Excited Tall Building," Second International Symposium on Structural Control, Univ. of Waterloo, Ontario, Canada, July 15-17, 1985.

41. Samali, B., Yang, J. N., and Liu, S. C., "Control of Lateral-Torsional Motion of Buildings under Seismic Load," Journal of Structural Engineering, Nov. 1985.

42. Shinozuka, M., and Li, D., "Optimal Motion Control of Open-bottom Floating Platforms," Technical Report, Columbia University, Feb. 1972.

43. Soong, T. T., Reinhorn, A. M., and Yang, J. N., "A Standardized Mode for Structural Control Experiments and Some Experimental Results," Second International Symposium on Structural Control, Univ. of Waterloo, Ontario, Canada, July 15-17, 1985.

44. Soong, T. T., and Skinner, G. T., "Experimental Study of Active Structural Control," Journal of the Engineering Mechanics Division, ASCE, Vol. 107, No. EM6, Dec. 1981, pp. 1057-1068.

45. Soong, T. T., and Chang, M. I. J., "On Optimal Control Configuration in Theory of Modal Control," Structural Control, edited by H. H. Leipholz, North-Holland Publishing Company, 1980, pp. 723-738.

46. Soong, T. T., and Chang, J. C. H., "Active Vibration Control of Large Flexible Structures," Shock and Vibration Bulletin, to appear.

47. Soong, T. T., et al, "Experimental Evaluation of Instantaneous Optimal Algorithms for Structural Control," National Center for Earthquake Engineering Research, Technical Report No. NCEER-87-0002, April 20, 1987.

48. Udwadia, F. E., and Tabaie, S., "Pulse Control of Structural and Mechanical Systems," Journal of the Engineering Mechanics Division, ASCE, Vol. 107, 1981, pp. 1011-1028.

49. Vilnay, O., "Design of Modal Control of Structures," Journal of the Engineering Mechanics Division, ASCE, Vol. 107, 1981, pp. 907-916.

50. Yang, J. N., "Application of Optimal Control Theory to Civil Engineering Structures," Journal of the Engineering Mechanics Division, ASCE, Vol. 101, No. EM6, Dec. 1975, pp. 818-838.

51. Yang, J. N., and Giannopoulos, F., "Active Tendon Control of Structures," Journal of the Engineering Mechanics Division, ASCE, Vol. 104, No. EM3, June 1978, pp. 551-568.

52. Yang, J. N., and Giannopoulos, F., "Active Control and Stability of Cable-Stayed Bridge," Journal of the Engineering Mechanics Division, ASCE, Vol. 105, No. EM4, Aug. 1979, pp. 677-694.

53. Yang, J. N., and Giannopoulos, F., "Active Control of Two Cable-Stayed Bridge," Journal of the Engineering Mechanics Division, ASCE, Vol. 105, No. EM5, Oct. 1979, pp. 795-810.

54. Yang, J. N., and Lin, M. J., "Optimal Critical-Mode Control of Building under Seismic Loads," Journal of Engineering Mechanics Division, ASCE, Vol. 108, No. EM6, Dec. 1982, pp. 1167-1185.

55. Yang, J. N., and Lin, M. J., "Building Critical-Mode Control; Non-stationary Earthquake," Journal of Engineering Mechanics Division, ASCE, Vol. 109, No. EM6, Dec. 1983, pp. 1375-1389.

56. Yang, J. N., "Control of Tall Buildings under Earthquake Excitations," Journal of the Engineering Mechanics Division, ASCE, Vol. 108, No. EM5, Oct. 1982.

57. Yang, J. N., and Samali, B., "Control of Tall Building in Along-Wind Motion," Journal of Structural Division, ASCE, Vol. 109, No. 1, Jan. 1983, pp. 50-68.

58. Yang, J. N., Akbarpour, A., and Ghaemmaghami, P., "Optimal Control Algorithms for Earthquake-Excited Buildings," paper to appear in the Proceedings of the 2nd International Symposium on Structural Control, University of Waterloo, Ontario, Canada, July 15-17, 1985.

59. Yang, J. N., Akbarpour, A., and Ghaemmaghami, P., "Instantaneous Optimal Control of Tall Buildings Under Seismic Loading," Presentation at the Third Specialty Conference on Dynamic Response of Structures, ASCE, Los Angeles, March 31-April 3, 1986.

60. Yao, J. T. P., and Abdel-Rohman, M., "Research Topics for Practical Implementation of Structural Control," Second International Symposium on Structural Control, Univ. of Waterloo, Ontario, Canada, July 15-17, 1985.

61. Yao, J. T. P., and Soong, T. T., "Importance of Experimental Studies in Structural Control," Reprint 84-010, ASCE, Atlanta Convention, May 14-18, 1984.

62. Yao, J. T. P., "Identification and Control of Structural Damage," Solid Mechanics Archives, Vol. 5, Issue 3, August 1980, pp. 325-345; Structural Control, edited by H. H. Leipholz, North-Holland Publishing Company, 1980, pp. 757-778.

63. Yao, J. T. P., and Sae-Ung, S., "Active Control of Building Structures," Journal of the Engineering Mechanics Divison, ASCE, Vol. 104, No. EM2, April 1978, pp. 335-350.

64. Yao, J. T. P., and Tang, J. P., "Active Control of Civil Engineering Structures," Technical Report No. CE-STR-73-1, Purdue University, 1973.

65. Yao, J. T. P., "Concept of Structural Control," Journal of the Structural Division, ASCE, Vol. 98, No. ST7, July 1972, pp. 1567-1574.

66. Yao, J. T. P., "Adaptive Systems for Seismic Structures," Proc. NSF-UCEER Earthquake Engineering Resources Conference, U. C. Berkeley, 1969, pp. 142-150.

67. Zuk, W., "Kinetic Structures," Civil Engineering, ASCE, Vol. 39, No. 12, 1968, pp. 62-64.

68. Zuk, W., and Clark, R. H., Kinetic Architecture, Van Norstrand Reinhold Co., N. Y., 1970.

69. Zuk, W., "The Past and Future of Active Structural Control Systems," Structural Control, edited by H. H. Leipholz, North-Holland Publishing Company, 1980, pp. 779-794.

70. Bryson, A. E., Jr., and Ho, Y. C., Applied Optimal Control, John Wiley and Sons, New York, 1975.

71. Yang, J. N., "Simulation of Random Envelope Processes," Journal of Sound and Vibration, Vol. 21, No. 1, 1972, pp. 73-85.

APPENDIX A

EQUATIONS OF MOTION

A.1 Equations Of Motion For Structures With An Active Tendon Control System

Let X_j be the displacement of the jth floor. For an active tendon control system in which a tendon controller can be installed between any two adjacent floors, see Fig. (2.1), the equation of the jth floor is given by

$$m_j \ddot{X}_j + c_j (\dot{X}_j - \dot{X}_{j-1}) - c_{j+1} (\dot{X}_{j+1} - \dot{X}_j)$$
$$+ k_j (X_j - X_{j-1}) - k_{j+1} (X_{j+1} - X_j)$$
$$+ \beta_j \dot{X}_j = u_{m+1} - u_m \qquad \text{For } j=1,2,\ldots, n \qquad (A.1)$$

in which m_j = mass of the jth floor, c_j = internal damping of the jth story unit, k_j = elastic stiffness of columns/shear walls of the jth story unit, and β_j = external damping. In Eq. (A.1), u_m is the control force from the mth controller that is installed between the j-1 and jth floors, and u_{m+1} is the control force from the m + 1th controller installed between the j and j+1th floors. Furthermore, $c_{n+1} = k_{n+1} = \beta_{n+1} = 0$.

Let X_0 be the earthquake ground displacement and y be the relative displacement of the jth floor with respect to the ground, i.e.,

$$Y_j = X_j - X_0 \qquad (A.2)$$

Then Eq. (A.1) can be written in a matrix form

$$\underset{\sim}{M} \, \ddot{\underset{\sim}{Y}} + \underset{\sim}{C} \, \dot{\underset{\sim}{Y}} + \underset{\sim}{K} \, \underset{\sim}{Y} = \underset{\sim}{H} \, \underset{\sim}{U} + \underset{\sim}{F} \, \ddot{X}_0 + \underset{\sim}{G} \, \dot{X}_0 \qquad (A.3)$$

in which

$$
\underset{\sim}{Y} = \begin{bmatrix} Y_1 \\ Y_2 \\ . \\ . \\ . \\ . \\ Y_n \end{bmatrix} ; \quad \underset{\sim}{U} = \begin{bmatrix} u_1 \\ u_2 \\ . \\ . \\ . \\ . \\ u_r \end{bmatrix} ; \quad \underset{\sim}{F} = - \begin{bmatrix} m_1 \\ m_2 \\ . \\ . \\ . \\ . \\ m_n \end{bmatrix} ; \quad \underset{\sim}{G} = - \begin{bmatrix} \beta_1 \\ \beta_2 \\ . \\ . \\ . \\ . \\ \beta_n \end{bmatrix} \quad (A.4)
$$

$$
\underset{\sim}{M} = \begin{bmatrix} m_1 & & & & & \\ & m_2 & & & & \\ & & \cdot & & & \\ & & & m_j & & \\ & & & & \cdot & \\ & & & & & \cdot \\ & & & & & & m_n \end{bmatrix} \quad (A.5)
$$

$$
\underset{\sim}{K} = \begin{bmatrix} k_1 + k_2, & -k_2 & , & 0 & & \\ -k_2, & k_2 + k_3, & -k_3 & & \\ & -k_3, & k_3 + k_4, & -k_4 & \\ & \cdot & \cdot & \cdot & \\ & & -k_{n-1}, & k_{n-1} + k_n, & k_n \\ & & & -k_n, & k_n \end{bmatrix} \quad (A.6)
$$

$$\underset{\sim}{C} = \begin{bmatrix} c_1+c_2+\beta_1, -c_2 & , & 0 \\ -c_2 & , c_2+c_3+\beta_2 , -c_3 \\ & -c_3 & , & c_3+c_4+\beta_3, & -c_4 \\ & & \cdot & \cdot & \cdot \\ & & \cdot & \cdot & \cdot \\ & & \cdot & \cdot & \cdot \\ & & & -c_{n-1}, & c_{n-1}+c_n+\beta_{n-1}, & -c_n \\ & & & & -c_n & , c_n+\beta_n \end{bmatrix} \qquad (A.7)$$

In Eq. (A.3), $\underset{\sim}{H}$ is an (n x r) location matrix whose mth column corresponds to the mth tendon controller installed between the j-1 and jth floor, i.e., jth story unit. This matrix can be obtained from a general (n x n) matrix $\underset{\sim}{L}$ by eliminating those columns that correspond to the story units without active tendon controller.

$$\underset{\sim}{L} = \begin{bmatrix} -1, 1 \\ & -1, 1 \\ & & \cdot & \cdot \\ & & & \cdot & \cdot \\ & & & & \cdot & \cdot \\ & & & & & \cdot & \cdot \\ & & & & & & \cdot & \cdot \\ & & & & & & & -1, 1 \\ & & & & & & & & -1 \end{bmatrix} \qquad (A.8)$$

Equation (A.3) can be expressed in terms of the 2n state vector $\underset{\sim}{Z}(t)$ as follows

$$\underset{\sim}{\dot{Z}}(t) = \underset{\sim}{A} \, \underset{\sim}{Z}(t) + \underset{\sim}{B} \, \underset{\sim}{U}(t) + \underset{\sim}{W}_1 \, \ddot{X}_0(t) + \underset{\sim}{W}_2 \, \dot{X}_0(t) \qquad (A.9)$$

in which

$$Z = \begin{bmatrix} Y \\ -- \\ \dot{Y} \end{bmatrix} \quad ; \quad A = \begin{bmatrix} 0 & \vdots & I \\ ---- & \vdots & ---- \\ -M^{-1}K & \vdots & -M^{-1}C \end{bmatrix} \quad (A.10)$$

$$B = \begin{bmatrix} 0 \\ --- \\ M^{-1}H \end{bmatrix} \quad ; \quad W_1 = \begin{bmatrix} 0 \\ --- \\ M^{-1}F \end{bmatrix} \quad ; \quad W_2 = \begin{bmatrix} 0 \\ --- \\ M^{-1}G \end{bmatrix} \quad (A.11)$$

A.2 Equations Of Motion For Structures With An Active Mass Damper System

Instead of the active tendon control system considered previously, a tall building implemented by an active mass damper shown in Fig. (3.7) is considered. The equation of motion for lower n-1 floors is:

$$m_j\ddot{X}_j + c_j(\dot{X}_j - \dot{X}_{j-1}) - c_{j+1}(\dot{X}_{j+1} - \dot{X}_j)$$

$$+ k_j(X_j - X_{j-1}) - k_{j+1}(X_{j+1} - X_j)$$

$$+ \beta_j\dot{X}_j = 0 \qquad \text{For } j=1,2,\ldots, n-1 \qquad (A.12)$$

and the equations of motion for the nth floor and the mass damper are, respectively,

$$m_n\ddot{X}_n + c_n(\dot{X}_n - \dot{X}_{n-1}) + k_n(X_n - X_{n-1})$$

$$- k_d(X_d - X_n) - c_d(\dot{X}_d - \dot{X}_n) + \beta_n\dot{X}_n = -u_d \qquad (A.13)$$

$$m_d\ddot{X}_d + c_d(\dot{X}_d - \dot{X}_n) + k_d(X_d - X_n) = u_d \qquad (A.14)$$

in which u_d = active control force, X_d = displacement of the mass damper, and m_d, c_d, and k_d = the mass, damping and the stiffness of the mass damper, respectively.

Let Y_d be the relative displacement of the mass damper with respect to the ground, i.e.,

$$Y_d = X_d - X_0 \qquad\qquad (A.15)$$

The equations of motion, Eqs. A.12-A.14, can be expressed in terms of the relative displacement in a matrix form

$$\underset{\sim}{M} \ddot{\underset{\sim}{Y}} + \underset{\sim}{C} \dot{\underset{\sim}{Y}} + \underset{\sim}{K} \underset{\sim}{Y} = \underset{\sim}{H} \underset{\sim}{U} + \underset{\sim}{F} \ddot{X}_0 + \underset{\sim}{G} \dot{X}_0 \qquad (A.16)$$

where

$$\underset{\sim}{Y} = \begin{bmatrix} Y_1 \\ Y_2 \\ \cdot \\ \cdot \\ \cdot \\ \cdot \\ Y_n \\ Y_d \end{bmatrix} \quad ; \quad \underset{\sim}{F} = - \begin{bmatrix} m_1 \\ m_2 \\ \cdot \\ \cdot \\ \cdot \\ \cdot \\ m_n \\ m_d \end{bmatrix} \quad ; \quad G = - \begin{bmatrix} \beta_1 \\ \beta_2 \\ \cdot \\ \cdot \\ \cdot \\ \cdot \\ \beta_n \\ 0 \end{bmatrix} \qquad (A.17)$$

$$\underset{\sim}{M} = \begin{bmatrix} m_1 & & & & & & \\ & m_2 & & & & & \\ & & \cdot & & & & \\ & & & \cdot & & & \\ & & & & m_j & & \\ & & & & & \cdot & \\ & & & & & & \cdot \\ & & & & & & \cdot m_n \\ & & & & & & & m_d \end{bmatrix}$$

$$, \quad \underset{\sim}{H} = \begin{bmatrix} 0 \\ 0 \\ \\ 0 \\ 0 \\ 0 \\ \\ 0 \\ 0 \\ 0 \\ -1 \\ 1 \end{bmatrix} \quad , \quad \underset{\sim}{U} = U_d \qquad\qquad (A.18)$$

$$\underset{\sim}{K} = \begin{bmatrix} k_1 + k_2, & -k_2 & , & 0 & & & \\ -k_2, & k_2 + k_3, & -k_3 & & & \\ & -k_3, & k_3 + k_4, & -k_4 & & \\ \cdot & & \cdot & & \cdot & \cdot \\ & \cdot & & \cdot & & \cdot \\ & \cdot & & & \cdot & \\ & & -k_{n-1}, & k_{n-1} + k_n, & -k_n & \\ & & & -k_n, & k_n + k_d, & -k_d \\ & & & & -k_d & , & k_d \end{bmatrix} \qquad (A.19)$$

$$
\underset{\sim}{C} = \begin{bmatrix}
c_1+c_2+\beta_1, & -c_2 & & , & 0 \\
-c_2 & , & c_2+c_3+\beta_2 & , & -c_3 \\
& & -c_3 & , & c_3+c_4+\beta_3, & -c_4 \\
& & \cdot & & \cdot & & \cdot \\
& & & \cdot & & \cdot & & \cdot \\
& & & & \cdot & & \cdot & & \cdot \\
& & & -c_{n-1}, & c_{n-1}+c_n+\beta_{n-1}, & -c_n \\
& & & & -c_n & , c_n+\beta_n, & -c_d \\
& & & & & -c_d & , & c_d
\end{bmatrix}
\qquad (A.20)
$$

Equation (A.16) can be expressed in terms of the state vector form as

$$
\dot{\underset{\sim}{Z}}(t) = \underset{\sim}{A}\ \underset{\sim}{Z}(t) + \underset{\sim}{B}\ \underset{\sim}{U}(t) + \underset{\sim}{W}_1\ \ddot{X}_0(t) + \underset{\sim}{W}_2\ \dot{X}_0(t) \qquad (A.21)
$$

where these matrices have the same form as those defined in Section 1, except that $\underset{\sim}{A}$ is a $(2n+1)$ by $(2n+1)$ matrix, and $\underset{\sim}{Z}$, $\underset{\sim}{B}$, $\underset{\sim}{W}_1$, and $\underset{\sim}{W}_2$ are $(2n+1)$ vectors.

APPENDIX B

OPTIMIZATION OF QUADRATIC PERFORMANCE INDEX

The problem of optimal control involves the determination of an appropriate vector, $U(t)$, which minimizes a performance index. A performance index widely used in the literature is the quadratic function as follows

$$J = \int_0^{t_f} \left\{ Z'(t) \ Q \ Z(t) + U'(t) \ R \ U(t) \right\} dt \qquad (B.1)$$

in which Q is a $(2n \times 2n)$ matrix that should be at least positive semi-definite, and R is a $(r \times r)$ positive definite matrix.

The differential equations of motion for the structural system is given by

$$\dot{Z}(t) = A \ Z(t) + B \ U(t) + W_1 \ddot{X}_0(t) \qquad (B.2)$$

with the initial condition

$$Z(0) = Z_0$$

where $Z(t)$ is a 2n-dimensional state vector and $\ddot{X}_0(t)$ is the ground acceleration.

To minimize the performance index given by Eq. (B.1) subjected to the constraint equations of motion represented by Eq. (B.2), these two equations are adjoined with the multiplier function $\lambda(t)$

$$\Im = \int_0^{t_f} \left\{ \left[\underset{\sim}{Z}'(t) \; \underset{\approx}{Q} \; \underset{\sim}{Z}(t) + \underset{\sim}{U}'(t) \; \underset{\approx}{R} \; \underset{\sim}{U}(t) \right] \right.$$

$$\left. + \underset{\sim}{\lambda}(t) \quad \left[\underset{\approx}{A} \; \underset{\sim}{Z}(t) + \underset{\approx}{B} \; \underset{\sim}{U}(t) + \underset{\sim}{W}_1 \; \ddot{\underset{\sim}{X}}_0(t) - \dot{\underset{\sim}{Z}}(t) \right] \right\} \; dt \qquad (B.3)$$

The integrand, that is a scaler function denoted by H, is referred to as the Hamiltonian,

$$H \left[\underset{\sim}{Z}(t), \underset{\sim}{U}(t), \underset{\sim}{\lambda}(t), \ddot{\underset{\sim}{X}}_0(t), t \right] =$$

$$\underset{\sim}{Z}'(t) \; \underset{\approx}{Q} \; \underset{\sim}{Z}(t) + \underset{\sim}{U}'(t) \; \underset{\approx}{R} \; \underset{\sim}{U}(t)$$

$$+ \underset{\sim}{\lambda}'(t) \quad \left[\underset{\approx}{A} \; \underset{\sim}{Z}(t) + \underset{\approx}{B} \; \underset{\sim}{U}(t) + \underset{\sim}{W}_1 \; \ddot{\underset{\sim}{X}}_0(t) - \dot{\underset{\sim}{Z}}(t) \right] \qquad (B.4)$$

where $\underset{\sim}{\lambda}(t)$ is a 2n-dimensinal vector representing the costate variables. Integrating by parts the last term of the right side of Eq. (B.3), and substituting Eq. (B.4) into Eq. (B.3), one obtains

$$\Im = -\underset{\sim}{\lambda}'(t_f) \; \underset{\sim}{Z}(t_f) + \underset{\sim}{\lambda}'(0) \; \underset{\sim}{Z}(0) +$$

$$\int_0^{t_f} \left\{ H \left[\underset{\sim}{Z}(t), \; \underset{\sim}{U}(t), \; \underset{\sim}{\lambda}(t), \; \ddot{\underset{\sim}{X}}_0(t), t \right] \right.$$

$$\left. + \dot{\underset{\sim}{\lambda}}'(t) \; \underset{\sim}{Z}(t) \right\} \; dt \qquad (B.5)$$

Taking the variation of $\Im$ yields

$$\delta\Im = -\underset{\sim}{\lambda}'(t_f) \; \delta\underset{\sim}{Z}(t_f) + \underset{\sim}{\lambda}'(0) \; \delta\underset{\sim}{Z}(0) +$$

$$\int_0^{t_f} \left[\left(\dot{\underset{\sim}{\lambda}}' + \frac{\partial H}{\partial \underset{\sim}{Z}} \right) \delta \underset{\sim}{Z} + \frac{\partial H}{\partial \underset{\sim}{U}} \delta \underset{\sim}{U} \right] \, dt \qquad (B.6)$$

The initiation condition $\underset{\sim}{Z}(0) = \underset{\sim}{Z}_0$ is a given constant state vector and hence $\delta \underset{\sim}{Z}(0) = 0$. Since Eq. (B.6) should be zero for any arbitary variations $\delta \underset{\sim}{Z}$ and $\delta \underset{\sim}{U}$, i.e., $\delta \tilde{J} = 0$, one has

$$\frac{\partial H}{\partial \underset{\sim}{U}} = 0 \quad , \quad 0 \leq t \leq t_f \qquad (B.7)$$

and

$$\dot{\underset{\sim}{\lambda}}' = -\frac{\partial H}{\partial \underset{\sim}{Z}} \qquad (B.8)$$

with the boundary conditions

$$\underset{\sim}{\lambda}'(t_f) = \underset{\sim}{0} \qquad (B.9)$$

substitution of Eq. (B.4) into Eqs. (B.7) and (B.8) results in the necessary conditions for the optimal solutions

$$\dot{\underset{\sim}{\lambda}} = -\underset{\sim}{A}' \underset{\sim}{\lambda} - 2 \underset{\sim}{Q} \underset{\sim}{Z} \quad , \quad \underset{\sim}{\lambda}(t_f) = \underset{\sim}{0} \qquad (B.10)$$

$$\underset{\sim}{U} = -0.5 \underset{\sim}{R}^{-1} \underset{\sim}{B}' \underset{\sim}{\lambda} \qquad (B.11)$$

The system of equations given by Eqs. (B.2), (B.10), and (B.11)
provide the optimal solutions for the control vector $U(t)$, the
response state vector $Z(t)$ and the costate vector $\lambda(t)$. It
should be noticed that the boundary conditions for Eqs. (B.2) and
(B.10) are different; the former are specified at $t = 0$ and the
latter are specified at $t = t_f$. This is a two-point boundary
value problem.

APPENDIX C
RANDOM VIBRATION OF STRUCTURES WITH AN ACTIVE CONTROL SYSTEM

With the application of the classical optimal control theory, the necessary conditions for the optimal control of a structure are obtained in the following.

$$\dot{\underset{\sim}{Z}}(t) = \underset{\sim}{A} \ \underset{\sim}{Z}(t) + \underset{\sim}{B} \ \underset{\sim}{U}(t) + \underset{\sim}{W}_1 \ \ddot{X}_0(t) \quad ; \quad \underset{\sim}{Z}(0) = 0 \qquad (C.1)$$

$$\dot{\underset{\sim}{\lambda}}(t) = - \ \underset{\sim}{A}' \underset{\sim}{\lambda}(t) - 2 \ \underset{\approx}{Q} \ \underset{\sim}{Z}(t) \qquad\qquad ; \quad \underset{\sim}{\lambda}(t_f) = 0 \qquad (C.2)$$

$$\underset{\sim}{U}(t) = - \ (1/2) \ \underset{\sim}{R}^{-1} \ \underset{\sim}{B}' \ \underset{\sim}{\lambda}(t) \qquad\qquad\qquad (C.3)$$

in which $\underset{\sim}{Z}(t)$ is the response state vector, $\underset{\sim}{U}(t)$ is the control vector, $\underset{\sim}{\lambda}(t)$ is the co-state vector and $\ddot{X}_0(t)$ is the earthquake ground acceleration. Note that Eq. (C.1) is nothing but the equation of motion of the structure with an active control system.

The earthquake ground acceleration can be modeled realistically as a stochastic process. It follows from Eqs. (C.1) to (C.3) that the response state vector $\underset{\sim}{Z}(t)$ and the control vector $\underset{\sim}{U}(t)$ are also stochastic processes. Hence, the random vibration approach will be used to determine the statistical moments of the response state vector $\underset{\sim}{Z}(t)$ and the control vector $\underset{\sim}{U}(t)$ in this Appendix.

C.1 Earthquake Ground Acceleration Model

The earthquake ground acceleration, $\ddot{X}_0(t)$, can be modeled as a uniformly modulated nonstationary random process,

$$\ddot{X}_0(t) = \psi(t) \ \ddot{X}(t) \qquad\qquad\qquad (C.4)$$

in which $\psi(t)$ is a deterministic non-negative envelope function, and $\ddot{X}(t)$ a stationary random process with zero mean and a power spectral density $\Phi_{\ddot{X}\ddot{X}}(\omega)$. A commonly used spectral density $\Phi_{\ddot{X}\ddot{X}}(\omega)$ for $\ddot{X}(t)$ given in the following is considered, although several different functional forms have been suggested in the literature,

$$\Phi_{\ddot{X}\ddot{X}}(\omega) = \frac{1 + 4\zeta_g^2(\omega/\omega_g)^2}{\left[1 - (\omega/\omega_g)^2\right]^2 + 4\zeta_g^2(\omega/\omega_g)^2} \cdot S^2 \qquad (C.5)$$

in which ζ_g, ω_g and S are parameters depending on the intensity and the characteristics of the earthquake in a particular location. Various types of envelope functions $\psi(t)$ have been used in the literature. A particular envelope function given in the following will be used

$$\psi(t) = \begin{cases} 0 & ; & t < 0 \\ (t/t_1)^2 & ; & 0 \le t \le t_1 \\ 1 & ; & t_1 \le t \le t_2 \\ \exp[-c(t-t_2)] & ; & t > t_2 \end{cases} \qquad (C.6)$$

where t_1, t_2 and c are parameters which should be selected appropriately to reflect the shape and the duration of the earthquake ground acceleration.

Physically, $\psi(t)$ describes the amplitude modulation, whereas the spectral density $\Phi_{\ddot{X}\ddot{X}}(\omega)$ specifies the frequency content of the earthquake ground acceleration $\ddot{X}_0(t)$.

C.2 Statistics Of The State Response Vector $\underset{\sim}{Z}(t)$ And The Control Vector $\underset{\sim}{U}(t)$

Since the earthquake ground acceleration $\ddot{X}_0(t)$ has a zero mean, the mean values of the state response vector $\underset{\sim}{Z}(t)$ and the active control vector $\underset{\sim}{U}(t)$ are zero. The mean square values of $\underset{\sim}{Z}(t)$ and $\underset{\sim}{U}(t)$ are identical to the variances $\sigma^2_{\underset{\sim}{z}}(t)$ and $\sigma^2_{\underset{\sim}{u}}(t)$, respectively. Let $\underset{\sim}{H}_z(\omega)$ and $\underset{\sim}{H}_u(\omega)$ be the frequency response vectors of $\underset{\sim}{Z}(t)$ and $\underset{\sim}{U}(t)$ due to a unit steady state ground acceleration, i.e.,

$$\left.\begin{aligned} \ddot{X}_0(t) &= e^{i\omega t} \\[2mm] \underset{\sim}{Z}(t) &= \underset{\sim}{H}_z(\omega)\, e^{i\omega t} \\[2mm] \underset{\sim}{U}(t) &= \underset{\sim}{H}_u(\omega)\, e^{i\omega t} \end{aligned}\right\} \qquad (C.7)$$

and $\underset{\sim}{h}_z(t)$ and $\underset{\sim}{h}_u(t)$ be the impulse response vectors due to ground acceleration $\ddot{X}_0(t) = \delta(t)$, i.e.,

$$\left.\begin{aligned} \ddot{X}_0(t) &= \delta(t) \\[2mm] \underset{\sim}{Z}(t) &= \underset{\sim}{h}_z(t) \\[2mm] \underset{\sim}{U}(t) &= \underset{\sim}{h}_u(t) \end{aligned}\right\} \qquad (C.8)$$

Then, the impulse response vectors are related to the frequency response vectors through the Fourier transform pair

$$h_z(t) = \frac{1}{2\pi} \int_{-\infty}^{\infty} H_z(\omega) \, e^{i\omega t} \, d\omega \qquad (C.9)$$

$$h_u(t) = \frac{1}{2\pi} \int_{-\infty}^{\infty} H_u(\omega) \, e^{i\omega t} \, d\omega \qquad (C.10)$$

The state response vector $Z(t)$ and the control vector $U(t)$ are related to the earthquake ground acceleration $\ddot{X}_0(t)$ through

$$Z(t) = \int_0^t h_z(\tau) \, \ddot{X}_0(t-\tau) \, d\tau \qquad (C.11)$$

$$U(t) = \int_0^t h_u(\tau) \, \ddot{X}_0(t-\tau) \, d\tau \qquad (C.12)$$

The cross-correlation matrix, $R_{zz}(t)$, of the response state vector is by definition

$$R_{zz}(t) = E\left[Z(t) \, Z'(t)\right] \qquad (C.13)$$

Substituting Eq. (C.4) into Eq. (C.11) and then into Eq. (C.13), one obtains

$$R_{zz}(t) = E\left[\int_0^t h_z(\tau_1) \, \psi(t-\tau_1) \, \ddot{X}(t-\tau_1) \, d\tau_1 \right.$$

$$\left. \int_0^t \psi(t-\tau_2) \, X(t-\tau_2) \, h_z'(\tau_2) \, d\tau_2 \right]$$

$$= \int_0^t \int_0^t \underset{\sim}{h}_z(\tau_1) \, \psi(t-\tau_1) \, R_{\ddot{X}\ddot{X}}(\tau_2-\tau_1)$$

$$\psi(t-\tau_2) \, \underset{\sim}{h}_z'(\tau_2) \, d\tau_1 \, d\tau_2 \qquad\qquad (C.14)$$

in which $R_{\ddot{X}\ddot{X}}(\tau)$ is the autocorrelation function of the stationary random process $\ddot{X}(t)$, i.e.,

$$R_{\ddot{X}\ddot{X}}(\tau) = E \, [\ddot{X}(t) \, \ddot{X}(t+\tau)] \qquad\qquad (C.15)$$

which is related to the corresponding power spectral density, $\Phi_{\ddot{X}\ddot{X}}(\omega)$, given by Eq. (C.5), through the Wiena-Khinchin's relation

$$R_{\ddot{X}\ddot{X}}(\tau_2-\tau_1) = \int_{-\infty}^{\infty} \Phi_{\ddot{X}\ddot{X}}(\omega) \, e^{i\omega(\tau_2-\tau_1)} \, d\omega \qquad\qquad (C.16)$$

Substitution of Eq. (C.16) into Eq. (C.14) yields

$$\underset{\sim}{R}_{zz}(t) = \int_{-\infty}^{\infty} \underset{\sim}{M}_z(t,\omega) \, \Phi_{\ddot{X}\ddot{X}}(\omega) \, \underset{\sim}{M}_z'(t,\omega) \, d\omega \qquad\qquad (C.17)$$

in which

$$\underset{\sim}{M}_z(t,\omega) = \int_0^t \underset{\sim}{h}_z(\tau) \, \psi(t-\tau) \, e^{-i\omega\tau} \, d\tau \qquad\qquad (C.18)$$

Since the mean value of the response state vector is zero, the covariance matrix is identical to the cross-correlation matrix $R_{zz}(t)$. The variance vector of $\underset{\sim}{Z}(t)$, denoted by $\sigma_z^2(t)$, is equal to the mean square vector, and the jth element of $\sigma_z^2(t)$ is equal to the jth diagonal element of $R_{zz}(t)$. Thus, the mean square response state vector is given by

$$\sigma_z^2(t) \quad = \int_{-\infty}^{\infty} |\underset{\sim}{M}_z(t,\omega)|^2 \; \Phi_{\dot{X}\dot{X}}(\omega) \quad d\omega \tag{C.19}$$

where $|\underset{\sim}{M}_z(t,\omega)|^2$ is a vector whose jth element is equal to the square of the absolute value of the jth element of $\underset{\sim}{M}_z(t,\omega)$ given by Eq. (C.18).

In a similar manner, the mean square vector of the active control force can be obtained as

$$\sigma_u^2(t) \quad = \int_{-\infty}^{\infty} |\underset{\sim}{M}_u(t,\omega)|^2 \; \Phi_{\dot{X}\dot{X}}(\omega) \quad d\omega \tag{C.20}$$

in which

$$\underset{\sim}{M}_u(t,\omega) = \int_0^t \underset{\sim}{h}_u(\tau) \; \psi(t-\tau) \; e^{-i\omega\tau} \quad d\tau \tag{C.21}$$

and the jth element of $|\underset{\sim}{M}_u(t,\omega)|^2$ is the square of the absolute

value of the jth element of $\underset{\sim}{M}_u(t,\omega)$ given in Eq. (C.21). It is mentioned that the quantities $|\underset{\sim}{M}_z(t,\omega)|^2 \Phi_{\ddot{X}\ddot{X}}(\omega)$ and $|\underset{\sim}{M}_u(t,\omega)|^2 \Phi_{\ddot{X}\ddot{X}}(\omega)$ in the integrand of Eqs. (C.19) and (C.20) are evolutionary spectra of $\underset{\sim}{Z}(t)$ and $\underset{\sim}{U}(t)$, respectively.

The numerical computation of the non-stationary root mean square vectors, $\underset{\sim}{\sigma}_z(t)$ and $\underset{\sim}{\sigma}_u(t)$, of $\underset{\sim}{Z}(t)$ and $\underset{\sim}{U}(t)$ can be carried out very efficiently in the following manner.

(i) The impulse response vectors $\underset{\sim}{h}_z(t)$ and $\underset{\sim}{h}_u(t)$ are computed from the corresponding frequency response vectors $\underset{\sim}{H}_z(\omega)$ and $\underset{\sim}{H}_u(\omega)$ from Eqs. (C.9) and (C.10) using the Fast Fourier Transform (FFT) technique.

(ii) $\underset{\sim}{M}_z(t,\omega)$ and $\underset{\sim}{M}_u(t,\omega)$ are computed from Eqs. (C.18) and (C.21) using the FFT technique.

(iii) The mean square vectors $\underset{\sim}{\sigma}_z(t)$ and $\underset{\sim}{\sigma}_u(t)$ are evaluated by numerically integrating the respective evolutionary spectral densities $|\underset{\sim}{M}_z(t,\omega)|^2 \Phi_{\ddot{X}\ddot{X}}(\omega)$ and $|\underset{\sim}{M}_u(t,\omega)|^2 \Phi_{\ddot{X}\ddot{X}}(\omega)$ and taking the square root. These numerical integrations are very simple and straight forward. Thus the computation of the non-stationary root mean square values of the structural response and the control force is nothing but repeated applications of the FFT technique which is very efficient.

C.3 Determination Of Frequency Response Functions

It follows from the random vibration analysis presented above that the frequency response vectors, $\underset{\sim}{H}_z(\omega)$ and $\underset{\sim}{H}_u(\omega)$, of $\underset{\sim}{Z}(t)$ and $\underset{\sim}{U}(t)$ should be determined. These frequency response vectors depend on the particular control law used. In this section, the frequency response vectors will be determined for the classical Riccati closed-loop control, the classical optimal open-loop control and the classical optimal closed-open-loop control. Note that for the latter two cases, a priori knowledge of the earthquake ground acceleration $\ddot{X}_0(t)$ is needed.

(a) Classical Riccati Closed-Loop Control

With the Riccati closed-loop control, the control vector is related to the measured response state vector $\underset{\sim}{Z}(t)$ through the Riccati matrix $\underset{\sim}{P}$

$$\underset{\sim}{U}(t) = - (1/2) \underset{\sim}{R}^{-1} \underset{\sim}{B}' \underset{\sim}{P} \underset{\sim}{Z}(t) \tag{C.22}$$

in which the time dependent Riccati matrix $\underset{\sim}{P}(t)$ is approximated by the constant Riccati matrix $\underset{\sim}{P}$.

Substitution of Eq. (C.22) into Eq. (2.1) yields

$$\dot{\underset{\sim}{Z}}(t) = \underset{\sim}{A}_1 \underset{\sim}{Z}(t) + \underset{\sim}{W}_1 \ddot{\underset{\sim}{X}}_0(t) \quad ; \quad \underset{\sim}{Z}(0) = 0 \tag{C.23}$$

in which

$$\underset{\sim}{A}_1 = A - (1/2) \underset{\sim}{B} \underset{\sim}{R}^{-1} \underset{\sim}{B}' \underset{\sim}{P} \tag{C.24}$$

Let $\Theta_1, \Theta_2, \ldots, \Theta_{2n}$ be the eigenvalues of the matrix $\underset{\sim}{A}_1$, and $\underset{\sim}{T}_1$ be the model matrix consisting of eigenvectors of $\underset{\sim}{A}_1$. Then, a transformation

$$\underset{\sim}{Z}(t) = \underset{\sim}{T}_1 \underset{\sim}{Y}(t) \tag{C.25}$$

in Eq. (C.23) will decouple the system of equations as follows

$$\dot{\underset{\sim}{Y}}(t) = \underset{\sim}{\Theta} \ \underset{\sim}{Y}(t) + \underset{\sim}{T}_1^{-1} \ \underset{\sim}{W}_1 \ \ddot{\underset{\sim}{X}}_0(t) \qquad (C.26)$$

where

$$\underset{\sim}{\Theta} = \begin{bmatrix} \ddots & & \\ & \Theta_j & \\ & & \ddots \end{bmatrix} = \underset{\sim}{T}_1^{-1} \ \underset{\sim}{A}_1 \ \underset{\sim}{T}_1 \qquad (C.27)$$

is a diagonal matrix consisting of diagonal elements Θ_j.

The jth equation of Eq. (C.26) can be written as

$$\dot{Y}_j(t) = \Theta_j \ Y_j(t) + g_j \ \ddot{X}_0(t) \qquad (C.28)$$

in which g_j is the jth element of the vector $\underset{\approx}{g} = \underset{\sim}{T}^{-1} \ \underset{\sim}{W}_1$.

The frequency response function is obtained when the excitation is a steady state sinosoidal, i.e.,

$$\left.\begin{array}{l} \ddot{\underset{\sim}{X}}_0(t) = e^{i\omega t} \\[2mm] \underset{\sim}{Z}(t) = \underset{\sim}{H}_z(\omega) \ e^{i\omega t} \\[2mm] \underset{\sim}{Y}(t) = \underset{\sim}{H}_y(\omega) \ e^{i\omega t} \\[2mm] Y_j(t) = H_{Y_j}(\omega) \ e^{i\omega t} \end{array}\right\} \qquad (C.29)$$

Application of Eq. (C.29) into Eq. (C.28) leads to the solution for $H_{Y_j}(\omega)$

$$H_{Y_j}(\omega) = g_j / [\Theta_j + \underset{\sim}{i} \omega] \quad ; \quad \text{for } j=1,2,\ldots \qquad \text{(C.30)}$$

Thus, the frequency response vectors $\underset{\sim}{H}_z(\omega)$ and $\underset{\sim}{H}_u(\omega)$ are obtained as

$$
\left.
\begin{aligned}
\underset{\sim}{H}_z(\omega) &= \underset{\sim}{T}_1 \, \underset{\sim}{H}_y(\omega) \\[2mm]
\underset{\sim}{H}_u(\omega) &= -\,(1/2)\, \underset{\sim}{R}^{-1} \, \underset{\sim}{B}' \, \underset{\sim}{P} \, \underset{\sim}{H}_z(\omega)
\end{aligned}
\right\} \qquad \text{(C.31)}
$$

(b) Classical Optimal Open-Loop Control

For the classical optimal open-loop control, the response state vector $\underset{\sim}{Z}(t)$ is not measured and

$$\underset{\sim}{\lambda}(t) = \underset{\sim}{g}(t) \qquad \text{(C.32)}$$

It follows from Eq. (C.2) that

$$\underset{\sim}{\dot{g}}(t) = -\underset{\sim}{A}' \, \underset{\sim}{g}(t) - 2 \, \underset{\sim}{Q} \, \underset{\sim}{Z}(t) \quad ; \quad \underset{\sim}{g}(t_f) = 0 \qquad \text{(C.33)}$$

Hence, $\underset{\sim}{Z}(t)$ and $\underset{\sim}{g}(t)$ should be solved from Eqs. (C.2) and (C.33), and then the control vector $\underset{\sim}{U}(t)$ is computed from $\underset{\sim}{g}(t)$ using Eq. (C.3), i.e.,

$$\underset{\sim}{U}(t) = -(1/2) \underset{\sim}{R}^{-1} \underset{\sim}{B}' \underset{\sim}{g}(t) \tag{C.34}$$

In order to solve for $\underset{\sim}{Z}(t)$ and $\underset{\sim}{g}(t)$, Eqs. (C.2) and (C.33) are written in a matrix equation as follows

$$\underset{\sim}{\dot{\xi}}(t) = \underset{\sim}{A}_2 \; \underset{\sim}{\xi}(t) + \underset{\sim}{W}_2 \; \underset{\sim}{\ddot{X}}_0(t) \tag{C.35}$$

in which $\underset{\sim}{\xi}(t)$ and $\underset{\sim}{W}_2$ are 4n vectors and $\underset{\sim}{A}_2$ is a (4n x 4n) matrix

$$\underset{\sim}{\xi}(t) = \begin{bmatrix} \underset{\sim}{Z}(t) \\ \hline \underset{\sim}{g}(t) \end{bmatrix} \; , \quad \underset{\sim}{A}_2 = \begin{bmatrix} \underset{\sim}{A} & \vdots & -(1/2)\,\underset{\sim}{R}^{-1}\,\underset{\sim}{B}' \\ \hline -2\underset{\sim}{Q} & \vdots & -\underset{\sim}{A}' \end{bmatrix} \; ,$$

$$\underset{\sim}{W}_2 = \begin{bmatrix} \underset{\sim}{W}_1 \\ \hline \underset{\sim}{0} \end{bmatrix} \tag{C.36}$$

Eq. (C.35) can be decoupled by the following transfomation

$$\underset{\sim}{\xi}(t) = \underset{\sim}{T}_2 \; \underset{\sim}{V}(t) \tag{C.37}$$

in which $\underset{\sim}{T}_2$ is the model matrix of the matrix $\underset{\sim}{A}_2$, i.e., the jth column of $\underset{\sim}{T}_2$ represents the jth eigenvector of $\underset{\sim}{A}_2$. Substitution of Eq. (C.37) into Eq. (C.35) leads to the uncoupled equations for $\underset{\sim}{V}(t)$, i.e.,

$$\underset{\sim}{\dot{V}}(t) = \underset{\sim}{\gamma} \; \underset{\sim}{V}(t) + \underset{\sim}{a} \; \underset{\sim}{\ddot{X}}_0(t) \tag{C.38}$$

in which $\underset{\sim}{\gamma}$ is a diagonal matrix such that the jth diagonal element γ_j is the jth eigenvalue of $\underset{\sim}{A}_2$ for j=1, 2, ..., 4n, i.e.,

$$\underset{\sim}{\gamma} = \left[{}_{\diagdown}\gamma_{j\diagdown} \right] = \underset{\sim}{T}_2^{-1} \underset{\sim}{A}_2 \underset{\sim}{T}_2 = \begin{bmatrix} \gamma_1 & & & & & 0 \\ & \ddots & & & & \\ & & \ddots & & & \\ & & & \gamma_j & & \\ & & & & \ddots & \\ & & & & & \ddots \\ 0 & & & & & \gamma_{4n} \end{bmatrix} \quad \text{(C.39)}$$

and

$$\underset{\sim}{a} = \underset{\sim}{T}_2^{-1} \underset{\sim}{W}_2 \quad \text{(C.40)}$$

The jth equation of Eq. (C.38) can be written as

$$\dot{V}_j(t) = \gamma_j V_j(t) + a_j \ddot{X}_0(t) \quad , \quad \text{for } j=1,2,\ldots,4n \quad \text{(C.41)}$$

where $V_j(t)$ and a_j are the jth elements of $\underset{\sim}{V}(t)$ and $\underset{\sim}{a}$, respectively. The frequency response functions given by

$$\left. \begin{aligned} &\ddot{X}_0(t) = e^{i\omega t} \quad , \quad \underset{\sim}{Z}(t) = \underset{\sim}{H}_Z(\omega) \, e^{i\omega t} \quad , \\[2mm] &\underset{\sim}{\xi}(t) = \underset{\sim}{H}_\xi(\omega) e^{i\omega t} \quad , \quad \underset{\sim}{V}(t) = \underset{\sim}{H}_V(\omega) \, e^{i\omega t} \quad , \\[2mm] &\underset{\sim}{V}_j(t) = H_{V_j}(\omega) \, e^{i\omega t} \end{aligned} \right\} \quad \text{(C.42)}$$

can be obtained in the following manner. Substituting Eq. (C.42) into Eq. (C.41), one obtains the frequency response function

$$H_{v_j}(\omega) = a_j \, / \, (\underset{\sim}{i} \, \omega - \gamma_j) \qquad\qquad (C.43)$$

Then, the frequency response vector $\underset{\sim}{H}_z(\omega)$ is obtained from Eq. (C.42) and the frequency response vector of $\underset{\sim}{U}(t)$ is determined from that of $\underset{\sim}{\xi}(t)$ and $\underset{\sim}{g}(t)$, see Eqs. (C.42), and (C.34) - (C.36).

(c) Classical Optimal Closed-Open-Loop Control

For the classical optimal closed-open-loop control, both the response state vector $\underset{\sim}{Z}(t)$ and the earthquake ground acceleration $\ddot{X}_0(t)$ are measured. Hence, the co-state vector $\underset{\sim}{\lambda}(t)$ is assumed to be

$$\underset{\sim}{\lambda}(t) = \underset{\sim}{P} \, \underset{\sim}{Z}(t) + \underset{\sim}{q}(t) \qquad\qquad (C.44)$$

in which the time dependent Riccati matrix $\underset{\sim}{P}(t)$ is approximated by the constant Riccati matrix $\underset{\sim}{P}$. Substituting Eq. (C.44) into Eqs. (C.1) through (C.3) yields

$$\underset{\sim}{\dot{q}}(t) = \underset{\sim}{A}_3 \, \underset{\sim}{q}(t) - \underset{\sim}{P} \, \underset{\sim}{W}_1 \, \ddot{X}_0(t) \quad ; \quad \underset{\sim}{q}(t_f) = 0 \qquad (C.45)$$

$$\underset{\sim}{\dot{Z}}(t) = \underset{\sim}{A}_4 \, \underset{\sim}{Z}(t) - (1/2) \, \underset{\sim}{B} \, \underset{\sim}{R}^{-1} \, \underset{\sim}{B}' \, \underset{\sim}{q}(t) \; +$$

$$\underset{\sim}{W}_1 \, \ddot{X}_0(t) \quad ; \quad \underset{\sim}{Z}(0) = 0 \qquad\qquad (C.46)$$

$$\underset{\sim}{U}(t) = - (1/2) \, \underset{\sim}{R}^{-1} \, \underset{\sim}{B}' \, [\underset{\sim}{P} \, \underset{\sim}{Z}(t) + \underset{\sim}{q}(t)] \qquad (C.47)$$

in which A_3 and A_4 are defined as

$$A_3 = - A' + (1/2) P B R^{-1} B'$$ (C.48)

$$A_4 = A - (1/2) B R^{-1} B' P$$ (C.49)

Let β_1, β_2, ... , β_{2n} be the eigenvalues of the matrix A_3 and T_3 be the modal matrix consisting of eigenvectors of A_3. Then a transformation

$$q(t) = T_3 \eta(t)$$ (C.50)

in Eq. (C.45) will decouple the system of equations as follows

$$\dot{\eta}(t) = \beta \eta(t) - T_3^{-1} P W_1 \ddot{X}_0(t)$$ (C.51)

where

$$\beta = \left[\begin{matrix} \ddots & \\ & \beta_j \\ & & \ddots \end{matrix} \right] = T_3^{-1} A_3 T_3$$ (C.52)

is a diagonal matrix consisting of diagonal elements β_j.

The jth equation of Eq. (C.51) can be written as

$$\dot{\eta}_j(t) = \beta_j \eta(t) + f_j \ddot{X}_0(t)$$ (C.53)

C-14

in which f_j is the jth element of the vector $\underset{\sim}{F} = \underset{\sim}{T}_3 \underset{\sim}{P} \underset{\sim}{W}_1$.

Let α_1, α_2, ..., α_{2n} be the eigenvalues of the matrix $\underset{\sim}{A}_4$. Then by a transformation

$$\underset{\sim}{Z}(t) = \underset{\sim}{T}_4 \underset{\sim}{Y}(t) \tag{C.54}$$

One can decouple Eq. (C.46) as follows

$$\dot{\underset{\sim}{Y}}(t) = \underset{\sim}{\alpha} \underset{\sim}{Y}(t) + \underset{\sim}{S} \underset{\sim}{\eta}(t) + \underset{\sim}{d} \ddot{X}_0(t) \tag{C.55}$$

in which $\underset{\sim}{\eta}(t)$ is the vector obtained in Eq. (C.51) and

$$\underset{\sim}{\alpha} = \begin{bmatrix} \ddots \alpha_j \ddots \end{bmatrix} = \underset{\sim}{T}_4^{-1} \underset{\sim}{A}_4 \underset{\sim}{T}_4 \tag{C.56}$$

is a diagonal matrix consisting of diagonal elements α_j. Matrices $\underset{\sim}{S}$ and $\underset{\sim}{d}$ are given as follows

$$\underset{\sim}{S} = - (1/2) \underset{\sim}{T}_4^{-1} \underset{\sim}{B} \underset{\sim}{R}^{-1} \underset{\sim}{B}' \underset{\sim}{T}_3 \tag{C.57}$$

$$\underset{\sim}{d} = \underset{\sim}{T}_4^{-1} \underset{\sim}{W}_1 \tag{C.58}$$

The jth equation of Eq. (C.56) can be written as

$$\dot{Y}_j(t) = a_j \, Y_j(t) + \Lambda_j(t) + d_j \, \ddot{X}_0(t) \tag{C.59}$$

where $\Lambda_j(t)$ is the jth element of the vector $\underset{\sim}{\Lambda}(t) = \underset{\sim}{S} \, \underset{\sim}{\eta}(t)$ and d_j is the jth element of the vector $\underset{\sim}{d}$.

The frequency response function given by

$$\left.\begin{aligned}
\ddot{X}_0(t) = e^{i\omega t} &\quad , \quad \underset{\sim}{q}(t) = \underset{\sim}{H}_q(\omega) \, e^{i\omega t} \quad , \\[2ex]
\underset{\sim}{\eta}(t) = \underset{\sim}{H}_\eta(\omega) \, e^{i\omega t} &\quad , \quad \eta_j(t) = \underset{\sim}{H}_{\eta_j}(\omega) \, e^{i\omega t} \quad , \\[2ex]
\underset{\sim}{Z}(t) = \underset{\sim}{H}_z(\omega) \, e^{i\omega t} &\quad , \quad \underset{\sim}{Y}(t) = \underset{\sim}{H}_Y(\omega) \, e^{i\omega t} \quad , \\[2ex]
Y_j(t) = H_{Y_j}(\omega) \, e^{i\omega t} &
\end{aligned}\right\} \tag{C.60}$$

can be obtained as follows. Substitution of Eq. (C.60) into Eq. (C.53) yields

$$H_{\eta_j}(\omega) = f_j \, / \, (i\omega - \beta_j) \tag{C.61}$$

By substituting Eqs. (C.60) and (C.61) into Eq. (C.59), one obtains the frequency response function

$$H_{Y_j}(\omega) = \frac{H_{\Lambda_j}(\omega) + d_j}{(i\omega - a_j)} \tag{C.62}$$

in which $H_{\Lambda_j}(\omega)$ is the jth element of the vector $\underset{\sim}{H}_\Lambda(\omega) = \underset{\sim}{S} \, \underset{\sim}{H}_\eta(\omega)$.

Thus, the frequency response vectors $\underset{\sim}{H}_q(\omega)$, $\underset{\sim}{H}_z(\omega)$ and $\underset{\sim}{H}_u(\omega)$ are obtained as

$$
\left.
\begin{aligned}
\underset{\sim}{H}_q(\omega) &= \underset{\sim}{T}_3 \ \underset{\sim}{H}_\eta(\omega) \\[2em]
\underset{\sim}{H}_z(\omega) &= \underset{\sim}{T}_4 \ \underset{\sim}{H}_y(\omega) \\[2em]
\underset{\sim}{H}_u(\omega) &= - (1/2) \ \underset{\sim}{R}^{-1} \ \underset{\sim}{B}' \ [\underset{\sim}{P} \ \underset{\sim}{H}_z(\omega) + \underset{\sim}{H}_q(\omega)]
\end{aligned}
\right\} \qquad \text{(C.63)}
$$

REPORT DOCUMENTATION PAGE	1. REPORT NO. NCEER 87-0007	2.	3. Recipient's Accession No. PB8 134333/AS
4. Title and Subtitle Instantaneous Optimal Control Laws for Tall Buildings Under Seismic Excitations			5. Report Date June 10, 1987
			6.
7. Author(s) J.N. Yang, A. Akbarpour and P. Ghaemmaghami			8. Performing Organization Rept. No.
9. Performing Organization Name and Address National Center for Earthquake Engineering Research State University of New York at Buffalo Red Jacket Quadrangle Buffalo, New York 14260			10. Project/Task/Work Unit No.
			11. Contract(C) or Grant(G) No. (C) NCEER 86-3021, ECE 86-07591 (G) ECE 85-21496
12. Sponsoring Organization Name and Address			13. Type of Report & Period Covered
			14.

15. Supplementary Notes

This research was conducted at George Washington University and was partially supported by the National Science Foundation.

16. Abstract (Limit: 200 words)

A critical review of classical optimal control algorithms is made with respect to the specific application of structural control under seismic loads. With the earthquake ground acceleration being the major source of continuous external disturbances, the Riccati closed-loop control does not satisfy the optimal condition. New optimal control algorithms are proposed herein, including the instantaneous optimal open-loop control, instantaneous closed-loop control and instantaneous optimal closed-open-loop control. These new control algorithms are aimed at developing feasible control algorithms that can easily be implemented, for applications to seismic-excited structures. Numerical examples are worked out to demonstrate the control efficiency of the proposed control algorithms.

17. Document Analysis a. Descriptors

b. Identifiers/Open-Ended Terms

OPTIMAL CONTROL
CONTROL ALGORITHMS
SEISMIC SIMULATION
DYNAMIC LOADS   DYNAMIC STRUCTURAL ANALYSIS

STRUCTURAL CONTROL
SEISMIC EXCITATION
OPEN-LOOP CONTROL
CLOSED-LOOP CONTROL
CLOSED-OPEN-LOOP CONTROL

c. COSATI Field/Group

18. Availability Statement Release unlimited	19. Security Class (This Report) unclassified	21. No. of Pages 112
	20. Security Class (This Page) unclassified	22. Price PC 19.95/96.95

(See ANSI–Z39.18)   See Instructions on Reverse   OPTIONAL FORM 272 (4–77)
(Formerly NTIS–35)
Department of Commerce